Using Light Detection and Ranging (LiDAR) Imagery To Model Radio Wave Propagation

Jason Michael Cash

Thesis submitted to the Faculty of
Virginia Polytechnic Institute and State University
In partial fulfillment of the requirements for the degree of

Master of Science
In
Geography

Dr. Laurence W. Carstensen Jr., Chair
Dr. James B. Campbell Jr.
Dr. Charles W. Bostian

Virginia Polytechnic Institute and State University
Blacksburg, VA 24061
March 20, 2003

Keywords: commshed, DEM resolution, GIS, LiDAR, line-of-sight, radio wave propagation, signal strength, wireless telecommunication

Using Light Detection and Ranging (LiDAR) Imagery To Model Radio Wave Propagation

Jason M. Cash

(**ABSTRACT**)

The purpose of this study was to determine if light detection and ranging (LiDAR) imagery could provide a significantly more accurate data set for modeling near line-of-sight (LOS) propagation at higher frequencies, specifically 27.810 GHz. than a USGS digital elevation model (DEM). In addition, the study tested for significant differences in LiDAR elevation data created at various resolutions ranging from 1 to 100 meters. Finally, this study examined the effects of various classification thresholds for transforming continuous signal strength measurements into LOS or non-LOS (NLOS) classifications used in determining prediction accuracy. The capability to transmit information via higher frequency wireless equipment requires a near LOS path between the transmitter and the antenna receiving the signal. USGS DEMs, commonly used in GIS programs to predict communication viewsheds (commsheds), represent the bare earth topography and do not reflect surface features such as vegetation and buildings. In actuality these surface features can significantly influence near LOS paths and therefore a data set that contains these features can greatly improve the ability to predict commshed areas. LiDAR is a form of active imagery that records both the bare-earth as well as these surface features, at a high resolution, making it well suited for wireless modeling applications. Results indicate that signal strength threshold classification has a direct influence on the accuracy of predicted commsheds across all resolutions. Secondly, LiDAR resolutions lower than 40m as well as bare-earth DEMs were unsuccessful in predicting an accurate commshed while LiDAR resolutions coarser than 15m provided significant predictions of equal accuracy. These results indicate that high resolution LiDAR is needed to accurately model commsheds but signal strength threshold classification determines which of these higher resolutions are significant.

Acknowledgments

I would like to thank the following individuals for their contributions and assistance in this study:

Dr. Bill Carstensen for all of his supervision and wisdom throughout this study as well as over my years as a graduate student in the Geography department. Like many other GIS students who have taken many of his classes, an academic bond has developed.

Tim Gallagher for his patience and willingness to help with data collection on an unusually warm day in November. My work would not have been possible without his guidance in radio wave propagation and wireless communication.

Dr. Jim Campbell and Dr. Charles Bostian for their support and direction they provided with this study.

The Center for Wireless Telecommunications (CWT), Department of Forestry, Shultz Dining Center, and Rick Reed for graciously allowing the use of their equipment.

My fellow graduate students for being there on those stressful days when I needed to unwind. Especially Sam and Brent, who took me in during my first year in graduate school and helped "show me the ropes" and Sara Beth and Leigh for the 'support group' we created in those last months.

And finally I would like to send my deepest thanks to my wife, Lisa, for all of her support throughout this study, the countless hours she spent keeping me company on my numerous trips to Wytheville, VA and repeatedly trying to convince me that her name should be on the front of this thesis as well – I love you.

Table of Contents

List of Figures

Chapter 1: Introduction & Objective

1.1 Introduction

As the applications and demand for higher frequency wireless communication continue to grow, there is an increased desire for more accurate modeling capabilities. As with most studies, the costs for a thorough accuracy assessment can be enormous, justifying the need to develop more accurate modeling that can result in reduced efforts and costs. LMDS, Local Multi-point Distribution Service, is a wireless access system using a broad band portion of the radio spectrum ranging from 27.5 to 31 GHz in frequency and designated specifically for higher frequency wireless communication. This service allows for two-way digital communication for voice, video, and high-speed data transfer of up to several gigabits per second (VT-LMDS Group). LMDS can support large amounts of digital data for applications such as real time video and voice communications or high-speed internet which have requirements that are exponential in comparison to today's dial-up modems (Weisman, 2000). More demand is being placed on all forms of communication including land-based lines such as fiber optics and DSL (digital subscriber line). The wireless industry is meeting this demand with broadband width at higher frequencies capable of supporting more information. One tradeoff for the ability to carry increased information at shorter millimeter wavelengths is that the signal loses its ability to penetrate certain features in the environment making it more closely resemble line-of-sight (LOS). Lower radio frequencies, such as AM/FM radio, have longer wavelengths, allowing them to penetrate certain features such as building walls or vegetation. As a radio frequency increases, the wavelength decreases down to millimeters, and becomes more influenced by features in the environment. Rose (2001) states that "signal quality can be significantly degraded or blocked by natural and man-made obstructions due to this band's relatively short wavelength" (p.8). Therefore as the wireless industry continues its growth, it must find ways to cope with these tradeoffs.

Although the increased influence of surface features in the environment can be viewed as a disadvantage, higher frequencies become more easily modeled. The higher the frequency, the more propagation begins to resemble LOS. "This means that, according to theory, if you can see one point from another visually (up to a certain

distance) then the 24 GHz signal will be received at that point with little to no added signal loss. Conversely, if a point cannot be seen from another point, then very little or no signal will reach the receiver (barring any reflections from smooth surfaces)" (Rose 2001, p.8). This LOS characteristic results in the wave's inability to penetrate and bend around features that might have been possible in lower frequencies, but can be modeled well by many geographic information systems (GIS). GIS programs have the ability to calculate viewsheds, "commsheds" when dealing with wireless communication, quite well. A viewshed can be created with two pieces of information: a chosen viewpoint and an elevation surface. The program starts with the viewpoint, considers the surrounding elevations, and calculates what areas can be seen from the chosen viewpoint. The ability to predict areas having LOS with the viewpoint makes it a choice program for modeling radio wave propagation at higher frequencies resembling LOS. "Given the LOS properties of the wavelength, a viewshed would show the zones able to receive data, called a communication viewshed or 'commshed'" (Dodd 2001, p.4).

It is therefore possible to use GIS as a tool to model commsheds transmitted by high frequency antennas. But as mentioned before, the GIS program needs two pieces of information. The user chooses a viewpoint, in this case the transmitter site, but the elevation data needs to be provided as well. The data, used by the program, is in raster or cell format and should be as accurate as possible. The more closely this elevation data resembles the 'true' environment, the more accurate it will be in its predicted commshed. The field of remote sensing then becomes a partner with GIS as an important component in modeling wireless communication. Elevation data can be created by a variety of methods, all having both advantages and disadvantages. Rose states "accuracy is a function of the source, spatial resolution (cell size), and method of creation" (Rose 2001, p.10). Many well-developed methods for creating elevation data do not include surface features that, as mentioned previously, can significantly influence higher frequency propagation. Therefore in order to model these commsheds more accurately, it is important to use elevation data that contains features such as vegetation and buildings. A relatively new form of imagery in remote sensing known as LiDAR, light detection and ranging, is well suited to deal with this issue. Unlike passive methods used in satellite and photogrammetric imagery, LiDAR actively emits a light pulse from the bottom of an

aircraft, measures the return time of reflected pulses, and calculates distance from the aircraft based on the speed of light. By measuring the pulse return time, the elevation of the surface that reflected the pulse can be determined. Millions of pulses are generated and measured within a relatively small area resulting in a highly accurate representation of the surface. In addition to providing high resolution, LiDAR pulses are reflected off all surface features above the ground producing an image that not only contains the elevation of the ground, but also holds information about surface features. The ability of LiDAR to very accurately represent the elevation of the 'true' environment should work well with a GIS program when modeling LOS. Therefore, this study brings together three distinct fields: wireless communication, GIS viewshed capabilities, and remote sensing LiDAR imagery.

1.2 Objective

The purpose of this study was to determine if the use of light detection and ranging (LiDAR) imagery in relation to a USGS digital elevation model (DEM) could provide a significantly more accurate data set for modeling near line-of-sight radio wave propagation at higher frequencies, specifically 27.810 GHz. The second part of this study wanted to determine if there was significant difference among varying resolutions of LiDAR data. Would LiDAR data at a 10m resolution provide the same result as LiDAR data at 75m? And if not, is there a statistically significant difference between them? The answer would help decide if using higher resolution LiDAR data, which can be more expensive to collect and requires more processing time, can provide the added accuracy to help justify these concerns. Finally, this study explored the issue of transforming measured signal strength into LOS or non-LOS (NLOS) to see if this classification process had any influence on the results. The study converted high-density LiDAR imagery of the Wytheville, VA area into 13 different resolution raster grids (1m, 2m, 4m, 5m, 10m, 15m, 20m, 25m, 30m, 40m, 50m, 75m, and 100m). In addition, 3 USGS grids were downloaded from the Internet at resolutions of 10m, 30m, and 100m resulting in a total of 16 grids. They were then used in the GIS program to calculate a predicted commshed. In order to determine the accuracy of these predictions, field data was collected and an accuracy assessment done. The exact location and specifications used in

the GIS program's predicted commshed was then re-created in Wytheville and measurements of the 'true' commshed were recorded. Because GIS algorithms provide a binary output (visible or non-visible), to test the accuracy of the predicted commsheds, signal strengths measured on the 'true' commshed needed to be converted into LOS or NLOS categories. This classification method is determined by comparing measured signal strength against the signal strength anticipated at each site, determining the difference, and assigning each location to a LOS or NLOS category. The threshold of allowable difference between expected signal strength and that which was measured is an important aspect when working with wireless equipment. A minimal degree of difference can exist simply due to equipment fluctuation and is often expected and therefore systems are designed with more power than needed to provide a 'margin' of confidence. Increased threshold differences directly influence what geographic areas of the commshed will be considered as LOS or NLOS. Therefore this study examined the influence of various threshold classifications on the accuracy of the resulting commshed predictions. Five thresholds were chosen: –3dB, -6dB, -9dB, -12dB, and visibility. Information on these 'true' commsheds could then be compared to each of the 16 predicted commsheds to determine their accuracy. Each comparison resulted in an error matrix, which would allow for analysis to determine overall accuracy for each commshed in addition to determining its accuracy above chance agreement (Khat). This Khat score, representing overall accuracy minus chance success, was then tested for significance, which resulted in a final evaluation for each individual prediction. The 16 resulting predictions were then compared against one another to determine similarities and difference between resolutions. Finally, the classification of the 'true' commshed using five different signal strength thresholds was examined.

Chapter 2: Literature and Research

This study brings together three areas of focus: higher frequency wireless communication, remote sensing capabilities of LiDAR imagery, and GIS for LOS modeling. Extensive literature currently exists on each of these fields separately yet little research can be found that ties all three together. This chapter will address each area, give a brief summary of its capabilities, and explain how it contributes to this study. The conclusion will define how each of these three distinct fields come together to address questions asked by this study.

2.1 Wireless Communication, LMDS, and LOS

People interact with electromagnetic energy on a daily basis. Examples include using the microwave oven to warm food, having your speed monitored on interstate by a radar gun, or making an emergency call for help using your cell phone. Although this energy has a multitude of uses, this study is interested in its ability to transmit information between two points. Wireless communication is achieved by transmitting energy as a sine wave, which varies in its frequency, or cycles per second. By manipulating this wave, information can be transmitted by either analog or digital transmission. A few familiar frequencies and their sources are shown below (Weisman, 2000).

FM Radio	88,000,000 Hertz	~88 MHz
Cellular Phones	824,000,000 Hertz	~824 MHz
Airborne Radar	9,000,000,000 Hertz	~9 GHz
LMDS	28,000,000,000 Hertz	~28 GHz
Visible Light	500,000,000,000,000 Hertz	~500,000 GHz

Included in this list is LMDS, Local Multi-point Distribution Service, which is a common frequency used in high-speed Internet service. The range of frequencies in which a given application can operate is defined by its bandwidth. The number of frequencies capable of operating within a given band increase as total bandwidth increases. More frequencies result in the potential to carry more information. To illustrate this point, consider that a

normal telephone conversation requires approximately 4kHz of bandwidth, which means that LMDS frequencies are capable of transmitting close to 250,000 telephone conversations at the same time (Weisman, 2000).

Within the United States, the Federal Communications Commission (FCC) is responsible for keeping all these various frequencies, bandwidths, and wireless signals in order, preventing confusion and conflicts from developing. Certain pre-defined bandwidth ranges are unlicensed and unregulated allowing uncontrolled access to those operating equipment within these frequencies. LMDS on the other hand, ranging from approximately 27 to 31 GHz, is a licensed band. Within a geographic area, LMDS bandwidth can be purchased in a manner similar to the way real estate would be purchased giving owner exclusive rights to operate in that region at LMDS frequencies. The wider the bandwidth, the more information the owner can transmit and thus far, the LMDS band is the widest band ever allocated by the FCC (Weisman, 2000).

Wireless signals are transmitted from one location to another through the use of different types of antennas. Antennas are designed to convert electrical current into a wireless signal, wireless signal into an electrical current, and sometimes both. The size and shape of the antenna is tailored to the frequency being used and the intended direction in which the signal will be travelling. Wavelength is inversely linked to the frequency used, therefore increases in frequency result in decreases in wavelength (figure 1). Higher frequencies used in LMDS communication correspond to millimeter sized wavelengths, resulting in relatively small antenna sizes.

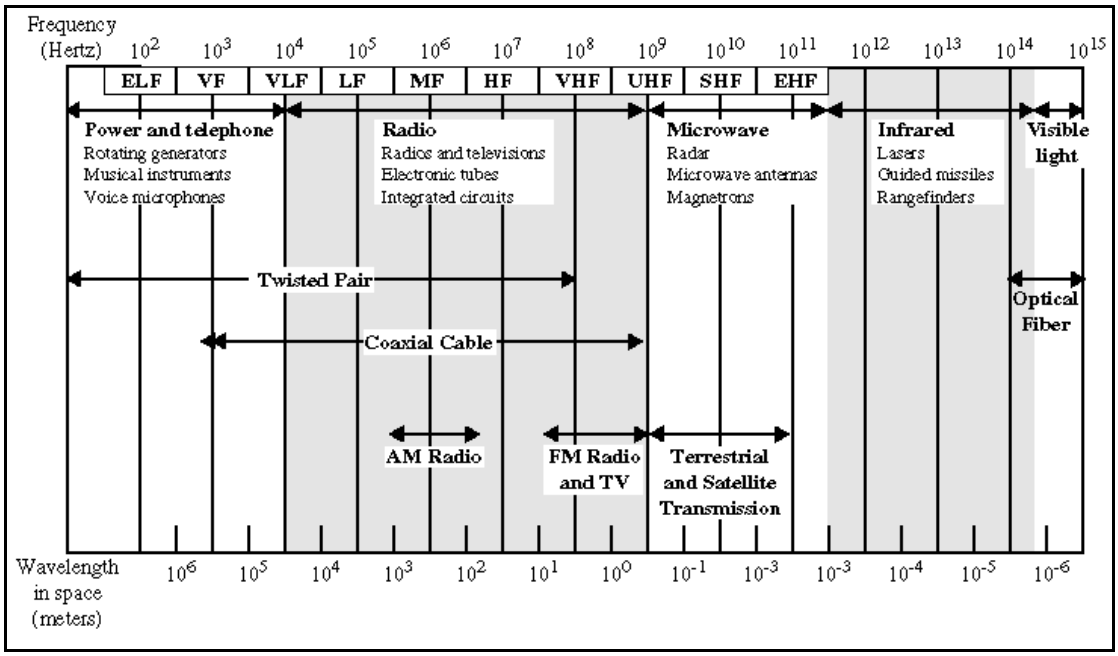

Figure 1.
The telecommunications industry operates at a range of frequencies. For example, broadcast radio communication uses a lower frequency while satellites and microwave systems use a much higher frequency. (Image courtesy of University of Wisconsin).

Omni-directional antennas are designed to transmit and receive signals in all directions while directional antennas are built to operate within a certain angular range (Weisman, 2000). Since a transmitter produces a limited amount of energy, the directional aspects of the antenna are critical to the distance the signal can travel. In addition to these directional properties, waves created by an antenna produce what is known as a fresnel zone. A fresnel zone is an area or 'envelope' surrounding the LOS path that the signal spreads out into as it travels away from the antenna. This predictable behavior of a signal is important because signal strength can be reduced when obstructions are blocking this 'envelope' even though LOS may exist between two points.

A consequence of decreased wavelength with higher frequencies is that signals become more influenced by the environment in which they are propagated. Weisman states "most of the 'things' the RF signal encounters tend to make the signal smaller, including the air we breathe, rain, glass, wood, and even foliage" (Weisman, p. 132). When portions of the signal are absorbed they lose strength, measured in decibels (dB), and therefore lose their ability to carry information. The increased influence of features

in the environment creates a characteristic known as line-of-sight (LOS). This means that, in order for information to travel from point A to point B via wireless communication, the two points must have mutual visibility between them. The significant influence of features in the environment makes it necessary to include them during the modeling process and is the basis for this study. It is important to address the terminology used in measuring, discussing, and comparing radio wave signal strength. When discussing the difference in power between two signals, values are referred to in decibels or dB. Values in dB are relative measurements and are not absolute. Signal strength differences would be calculated using the following formula.

$$dB = 10 \cdot \log_{10}\left(\frac{p_1}{p_2}\right)$$

where p_1 and p_2 are the two powers to be compared and dB is decibels.

Interest in absolute signal power occurs when using equipment to record the signal's strength and values are referred to in dBm. As an example, a 10 dBm would mean 10 dB above 1 mW. The formula below shows how to calculate absolute signal power.

$$dBm = 10 \cdot \log_{10}\left(\frac{p_1(mW)}{1mW}\right)$$

where p is power, mW is a milliwatts,
and dBm is decibel milliwatts.

The fundamental difference between both should be understood and will appear throughout this study.

2.2 LiDAR

LiDAR, Light Detection and Ranging, is an active form of remote sensing that records the travel time of light pulses to accurately measure surface elevation in a relatively small geographic region. The pulse-emitting equipment is mounted on the underside of an aircraft, typically a small plane, but helicopters can been used as well. The use of laser pulses (Light Amplification by Stimulated Emission of Radiation) to determine distance is made possible by the constant speed of light at 3 × 10^8 meters per

second. The LiDAR system emits a pulse of light directly down at the surface below and records the time it takes for this pulse to return after reflection from the surface (figure 2).

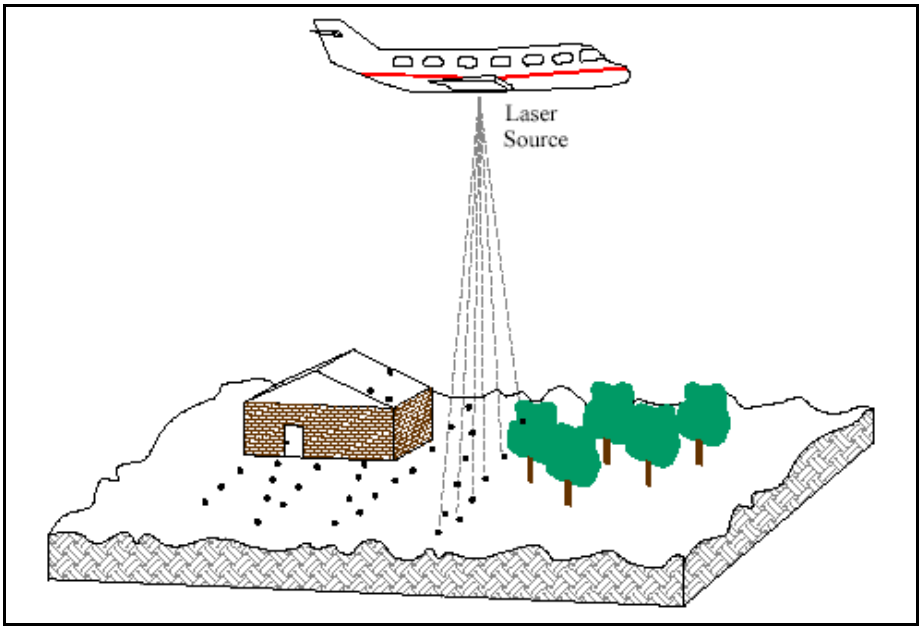

Figure 2.
LiDAR pulses are emitted downward, reflect off the surface, and return back to the aircraft. The total travel time of the pulse is then recorded and used to determine elevation. (Image courtesy of Gagne, 2001).

Once the return time has been measured, the following formula can be used to determine the complete distance between the LiDAR instrument and the surface.

$$\text{Distance} = c \text{ (speed of light)} \times t \text{ (recorded time)}$$

This distance is then subtracted from the aircraft's elevation above sea level, providing a final surface elevation for that pulse. "These systems use high-intensity laser instruments in conjunction with a variety of positioning and timing devices to directly determine the distance from the light source to an object" (Gagne 2001, p.21).

LiDAR collection is made possible using a variety of components, all meeting a certain level of accuracy. The following is a list of these components (Gagne, 2001).

LiDAR Equipment (generating laser pulses)

Global Positioning System (GPS)

Inertial Measurement System (IMU)

Camera or Video Recording Equipment

Powerful Computer

Hyper-accurate Master Clock

The LiDAR equipment creates pulses using an emitting diode. It is capable of generating hundreds to thousands of laser pulses within nanoseconds. A rotating mirror inside the system is then used to scan these pulses across the surface, creating a swath pattern (figure 2). A pulse originating from the instrument increases in diameter as it leaves the aircraft, illuminating a small area as opposed to a point when it finally reaches the surface. Depending on the flying altitude, angle, and speed of the aircraft, this area can be close to .3 meters in diameter by the time it reaches the ground (Gagne, 2001). This pulse area will then reflect from the surface but this surface may or may not be uniform. As an example, an area created by a pulse may partially reflect off the top of a tree, middle portions of the tree, and eventually the ground (figure 3). These multiple surfaces result in multiple pulse returns reflected back to the aircraft.

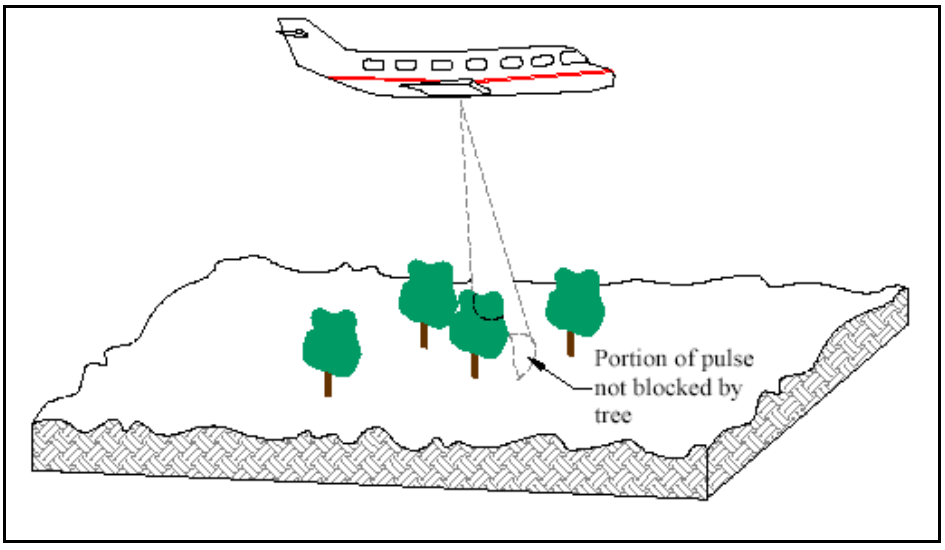

Figure 3.
As an individual pulse approaches the surface it increases in diameter. The resulting area covered by one pulse may then have multiple returns back to the aircraft based on the reflected surface. (Image courtesy of Gagne 2001).

As a result a single pulse can create multiple returns, due to different heights of features in the environment. The equipment can then record multiple returns for a single pulse. One can imagine the amount of information stored with thousands of pulses generated each nanosecond and each having multiple returns.

This surface elevation is only partially useful unless its location is known as well. GPS units mounted on the LiDAR equipment help to determine the exact position and orientation of the aircraft during pulse generation. In addition, small changes in the aircraft's orientation and airspeed, required for straight flight lines, need to be accounted for as well. Orientation of the aircraft include pitch, roll, and yaw (crawl) and are defined as "pitch is the rotation of the plane about its x-axis, roll is the plane about its y-axis, and yaw … is the rotation of the plane about its z-axis" (Gagne 2001, p.24). All three factors have a significant influence on the direction and angle of pulses generated from the LiDAR equipment (figure 4).

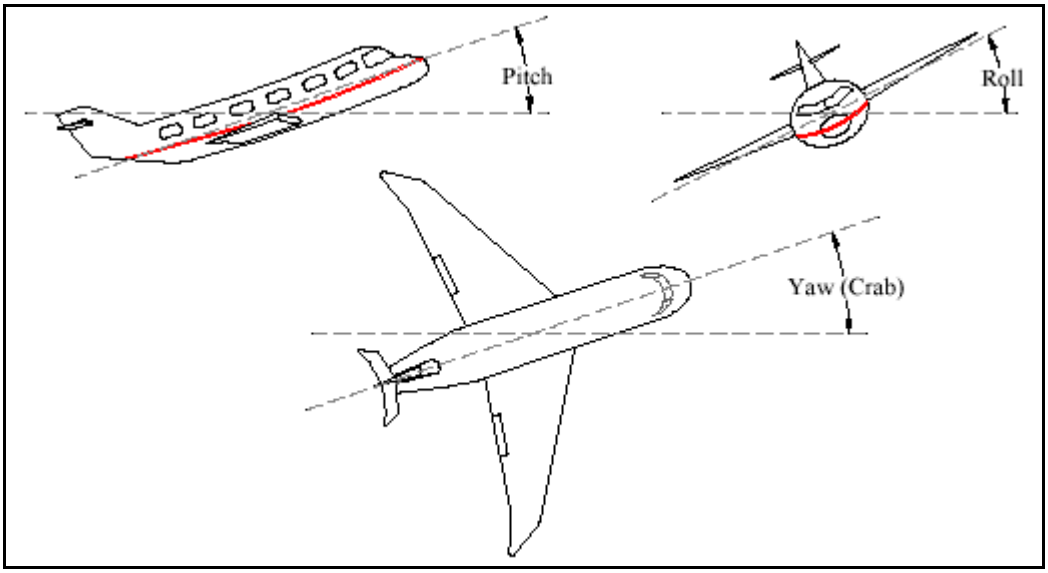

Figure 4.
Three common parameters effecting an aircraft can influence LiDAR collection.
(Image courtesy of Gagne 2001).

These factors are accounted for by using an Inertial Measurement Unit (IMU). The IMU includes a gyroscope and an accelerometer, which accurately measures any changes in the aircraft's orientation (Gagne 2001). Finally, all previously mentioned components of the LiDAR system require highly precise measurements of timing that can be

synchronized using a master clock. This is important because small discrepancies in timing can result in large errors in the final elevation data.

LiDAR data provides a highly accurate source of elevation that represents either the bare-earth, surface features, or both. This study was strictly interested in the first return provided by each LiDAR pulse, which can represent the bare-earth in open areas or the vegetation and buildings in other areas. LMDS frequencies are influenced by almost anything in the environment such as vegetation and buildings. Since LiDAR uses wavelengths close to visible light, pulses are reflected by everything in the environment excluding water bodies. LiDAR data therefore contains all of these surface features that may have an influence on LMDS signals. This study wanted to determine if the more accurate elevation data provided by LiDAR is more useful than simple bare-earth DEMs in modeling LMDS frequency propagation.

2.3 GIS and LOS Viewsheds

A geographic information system is a tool that is capable of combining and analyzing a multitude of geographic and attribute data to answer questions and address problems. One of its strengths is that it has the ability to calculate line-of-sight (LOS). By choosing a single point on a map, the program can highlight a viewshed on the map that can be seen from this chosen point. LOS calculations based on grids require two pieces of information: one is for the user to choose the initial viewpoint, the second is data that contains elevation data in grid format. This grid, similar to an image file, consists of regularly spaced cells with consistent dimensions. The program is able to start at the viewpoint, look at each surrounding cell's elevation, and then determine if it has LOS with the viewpoint (figure 5).

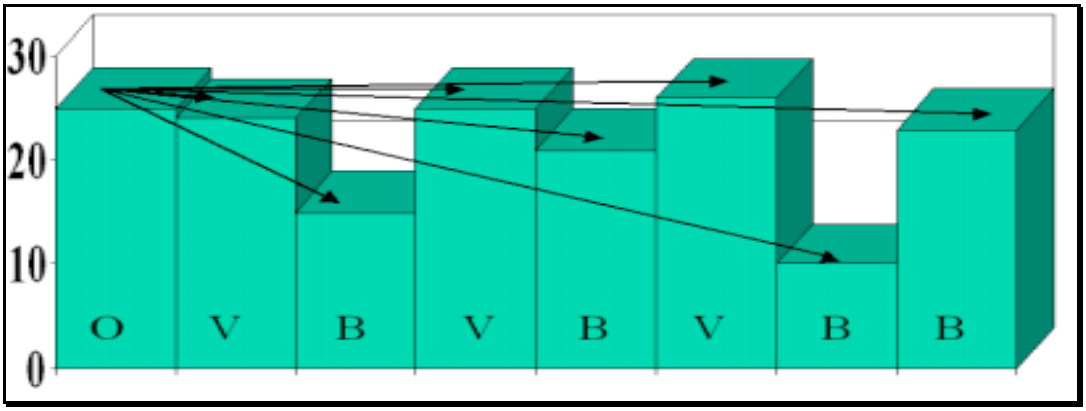

Figure 5.
LOS is calculated by looking at adjacent cells, determining LOS, then continues to surrounding cells. The example above shows how each cell is then classified as 'visible' or 'blocked.' (Image courtesy of Leach, 2001)

It then looks at adjacent cells, compares the angle from the viewpoint to the first cell against the angle from the first cell to the second and determines if the second cell has LOS. This process continues until all cells in the grid are assigned either LOS or not. There are a variety of methods the GIS program can work with when dealing with elevation data and all have their own advantages and disadvantages. These methods include "linear interpolation between grid neighbors, triangulation of the grid, grid constraints of the DEM mesh, and the stepped model" (Dodd 2001, p.6). Details on each of these methods is beyond the scope of this study but Dodd labels the stepped method as the most conservative and the linear interpolation between grid neighbors as the most generous in calculating LOS. The manner in which the program determines the exact origin and target position for each cell in the grid can also be a potential source for error. Each cell can be defined as its center point or its bounding outside corners. When determining LOS, the program can use either or a combination of both. It is important to address these two issues for the reader to understand that no method is absolute and each has its own advantages. Dodd (2001) indicates that computing LOS between all corners of the origin cell versus all corners of the target cell will provide the largest possibility for having LOS. Using the center point for both the origin and target cells will produce the most stringent viewshed.

A GIS program's ability to compute LOS can be used for LMDS propagation modeling. Modeling viewsheds of radio frequencies is referred to as communication

viewsheds or commsheds. Since LMDS radio waves have LOS characteristics, GIS becomes a powerful modeling tool.

2.4 Bringing it all together: LMDS, LiDAR, and GIS

Three separate fields have been addressed thus far. This includes the characteristics of radio frequencies and antenna design, LiDAR elevation data, and finally GIS abilities to model LOS. A combination of these three areas is the basis for this study. The overall goal is to determine if LiDAR imagery used in a GIS program can accurately model LMDS radio wave propagation. We know that higher frequency radio waves such as those used in LMDS communication closely resemble line-of-sight and are highly influenced by vegetation and structures. We also know that GIS has the ability to calculate LOS and therefore works well in modeling LMDS frequencies. Finally, we know that LiDAR imagery contains highly accurate information in regards to the surface elevation. It is then possible to use this detailed LiDAR data with a GIS program as a tool for predicting LOS, resulting in a more accurately modeled commshed for LMDS signals.

The current wireless communication industry is beginning to use GIS to more successfully bring their products to the public. "Companies have an insatiable appetite for more detailed maps that enable them to tweak their systems and upgrade their quality of service" (Corbley 1997, p.2). Much of the industry uses 'clutter maps', in addition to other sources of information, to evaluate how the wireless signal propagated by their company will react in a particular environment. These 'clutter maps' showing land cover classifications are derived from aerial photography or satellite imagery and simply indicate certain types of environments. A 'clutter map' may show a certain area to be mostly fields where a signal may travel unobstructed while other areas may be heavily forested indicated a more difficult area to transmit a signal. The design software then reads the resulting map and provides the user with an approximation on how the well the signal will travel within a given environment (Corbley, 1997). In addition to 'clutter maps' containing information on land cover, many companies also use high resolution DEMs to provide information on elevation. More detailed maps allow wireless companies to more accurately site cellular towers in addition to gaining a better

understanding of how the signal will react within the environment. Better modeling in the office can save time and money by optimizing cellular network design and minimizing post-installation problems. Using a higher accuracy map in network design brings wireless companies "better service and happier customers, which translates directly into greater market share in an extremely competitive industry" (Corbley 1997, p. 3). Those working to model wireless networks must also deal with working with data that is not always current (Ohlson, 1995). In urban settings new buildings are always being constructed and vegetation is constantly changing. Photography and imagery are only snapshots of time, recording the earth's surface at an exact moment. Collecting recent and more updated information can be timely and expensive. Therefore, the wireless industry must deal with an ever-changing world.

The time and cost issues surrounding LiDAR need to be addressed as well. Advantages to using LiDAR include quick turnaround time and simplicity of data acquisition. The processing time required to transform raw LiDAR into a functional format is extremely quick sometimes resulting in usable data within hours of flight completion. In addition, LiDAR data can be recorded easily during day or night without possible weather constraints, reducing flight preparation time and can be a powerful advantage in dealing with emergency situations. A profound example includes the use of LiDAR after the 9/11 attacks where a substantial amount of communication infrastructure was destroyed and a need for quick assessment was critical. Fewer constraints in flight planning also allow companies to acquire the most updated information. The world is constantly changing especially in urban areas where building construction is an on going process. It is difficult to provide accuracy when data is continuously being outdated but the ease of acquiring LiDAR can be one solution to minimizing this problem. In comparison to traditional photogrammetric methods of obtaining building footprints and elevation data, LiDAR can be a cost-effective alternative as well. LiDAR's disadvantages are seen in situations where the accuracy it can provide may not be necessary. Aside from modeling higher frequency radio wave propagation, a desired level of accuracy may be provided through simple and inexpensive bare-earth DEMs. Still, the accuracy provided by LiDAR can be found in a host of applications ranging from flood control mapping to atmospheric changes.

Chapter 3: Methodology

3.1 Location of Study

The location for this study was the town of Wytheville, centrally located within Wythe County in southwestern Virginia. Wytheville was chosen because LiDAR imagery already existed for this area. In 2002, the Virginia Department of Transportation (VDOT) was involved in an I-81/I-77 relocation study to address the growing volume of traffic traveling through this corridor area adjacent to the town. Part of this study involved acquiring LiDAR data to aid in the decision process. The Virginia Tech Department of Civil and Environmental Engineering was involved, by creating 3D visualizations using the acquired LiDAR imagery to increase community interest. Due to Virginia Tech's involvement, VDOT donated the LiDAR data to the school for educational research purposes (figure 6).

Figure 6.
The LiDAR imagery covered a small portion of Wythe County. The complete data set consisted of over 16 million points (area outlined in green). A 2km by 2km area that held close to 700,000 points was chosen as a subset (area outlined in blue).

3.2 Preparing the LiDAR Data

The LiDAR data initially needed to be manipulated so that it could be used for this study. Ryan Spencer, a master's student working in the Geography Department at Virginia Tech, performed much of this initial manipulation. The original imagery began in 6 separate *.xyz files, containing latitude, longitude, and elevation data for every point. These points covered a much larger area than was needed for this study, therefore ESRI's ArcGIS program was used to display and select out a 2km x 2km area. Digital Orthophoto Quarter Quadrangles (DOQQs) were used during this process to find a diverse landscape containing buildings, roads, vegetation, and open fields. A Triangulated Irregular Network (TIN) was then created using all points within the 2km by 2km study area. The high density of points created a very detailed surface map of the area (figure 7). Spencer (2001) noted that certain gaps were apparent due to either lack in flight line overlap or LiDAR's inherent absorption by water bodies. This did not present a problem because this study was performed in an even smaller area within this 2 sq. km area and would avoid these less accurate areas.

Figure 7.
Triangulated Irregular Network (TIN) created from the LiDAR imagery.
(Elevation is shown as increasing from blue to red)

Using this TIN, Spencer created 13 grids with the following resolutions: 1-meter, 2m, 4m, 5m, 10m, 15m, 20m, 25m, 30m, 40m, 50m, 75m, and 100m (examples shown in figure 8, complete set in Appendix A). All grids were then projected into UTM coordinates to be used in the analysis.

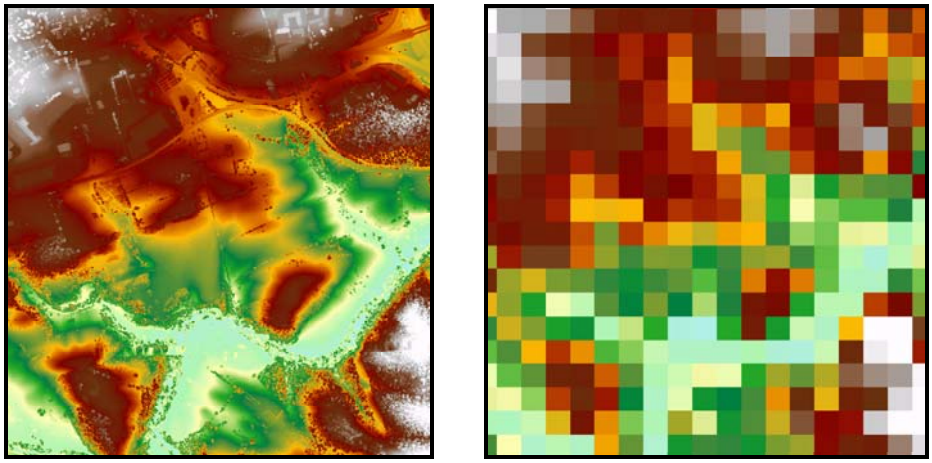

Figure 8.
The resulting 13 grids varied visually in their resolution.
The 1-meter and 100-meter examples above help to illustrate this point.

Spencer's 13 grids are the basis for this study. Three USGS DEM's were downloaded from the Internet to compare accuracy provided by LiDAR against that of a bare-earth DEM. These bare-earth only grids were 10m, 30m and 100 meters in resolution and did not contain any above ground features, as did the LiDAR grids. Once the three bare-earth grids were downloaded, they were projected from latitude/longitude into UTM coordinates to match the previous grids. A total of 16 grids were prepared and ready for analysis. See Appendix A.

3.3 Equipment

The Center for Wireless Telecommunications (CWT) provided the following signal strength equipment: a transmitter used to generate a LMDS signal, and a receiver to record this signal. The transmitter included a power source (AC outlet), a signal generator (Hewlett-Packard 8648C) propagating a wireless signal at 27.810 GHz, and a

horn antenna, which aims the signal in a given direction. The receiver included a deep cycle 12-volt marine battery to supply power, a spectrum analyzer (Hewlett-Packard 8594E) to measure the strength of the received signal, and another receiver antenna. A Micro-Corvallis March II-E 3.7 Global Positioning System (GPS) unit was used to record the exact location at which each measurement was taken (figure 9).

Figure. 9
On the left is the Hewlett-Packard 8648C signal generator and on the right is the Hewlett-Packard 8594E spectrum analyzer. (Image courtesy of Avalon Equipment Corporation)

3.4 Data Collection

In order to determine how accurately my 16 grids would predict a commshed, I needed to know the actual commshed. This required creating a real or 'true' commshed within my study area by setting up all previously mentioned equipment. I would collect data within this commshed using the spectrum analyzer, measuring signal strength at each site. The first step was to find a location within the 2km by 2km area covered by the 16 grids that would be suitable to set up the transmitter for this commshed. Ideal transmitter locations include spots that are well elevated, such as building roofs, which can provide a larger commshed with fewer objects blocking the generated signal. Finding this ideal location within my predefined grid area proved to be more difficult than expected. Previous work done by Virginia Tech on wireless communication used campus buildings, which did not present a problem. Unfortunately, the businesses in my study area were reluctant to allow access to their roofs for liability issues, thus as an alternative I was able to locate a well-elevated and open hill in the area. I was also able

to persuade the owner of the adjacent apartment building to allow the use of his electricity to power my transmitter equipment (figure 10).

Figure. 10
The top view, consisting of three images taken with a digital camera,
shows the area being targeted by the transmitter's commshed.
The second image shows a nearby apartment building used to power the transmitter.

Once the transmitter location was chosen, all preparations had been made to begin collecting data. Tim Gallagher, a PhD student working for the CWT, offered his expertise to help with equipment setup and data collection. The first step was to set up the transmitter at the chosen location. This included running extension cords to the nearby apartment building for power, setting up tables to support the equipment, and connecting all the transmitter parts together. The second step was to prepare the receiver equipment that Tim and I would be walking around with as we recorded signal strengths. In order to make the entire receiver equipment portable, a garden cart was purchased that would allow the equipment to be moved around as easily as possible. A marine deep cycle battery was also purchased to power the receiver. Once all parts of the receiver were connected and the GPS had initialized itself, I was ready to begin collecting data.

In trying to determine if LiDAR created grids containing information on vegetation and buildings could predict a more accurate commshed it was necessary to make sure my sample locations addressed this issue. As opposed to more traditional sampling methods such as random or stratified random, this study needed a approximately equal number of samples that fell within four categories: behind vegetation, behind buildings and structures, in open areas, and behind hills and terrain. Random sampling methods could not guarantee an even distribution into these categories and might possibly have suggested a number of inaccessible sample sites due to private property and public roadways where measurements were impossible. A stratified sampling method was chosen and sample locations were selected in the field as data was collected. Initial measurements began in open areas close to the transmitter but as the measurement equipment was moved around, data was collected behind buildings and vegetation. I was able to record data at 101 sites within the commshed using these four predefined sampling categories. The basic procedure for collecting data at each site was as follows:

1. The GPS unit was used to record the exact geographic location and the appropriate location number was entered into the unit.
2. A note was made as to whether or not the transmitter was visible or whether it was partial or completely blocked. Reasons were noted if it was blocked (i.e. vegetation, building, both).
3. A digital camera was used to record an image looking back at the transmitter from that site. These images were taken for reference during data analysis if necessary.
4. Finally, the receiver antenna was angled directly at the transmitter and slightly adjusted to obtain the strongest signal strength on the spectrum analyzer. This strength (dBm) was then noted (see Appendix B for complete field data).

It is important to understand how a wireless signal is transmitted when creating a commshed. The generated signal does not always radiate equally in all directions but does has a predictable pattern based on the transmitter, antenna pattern, and the signal frequency (figure 11).

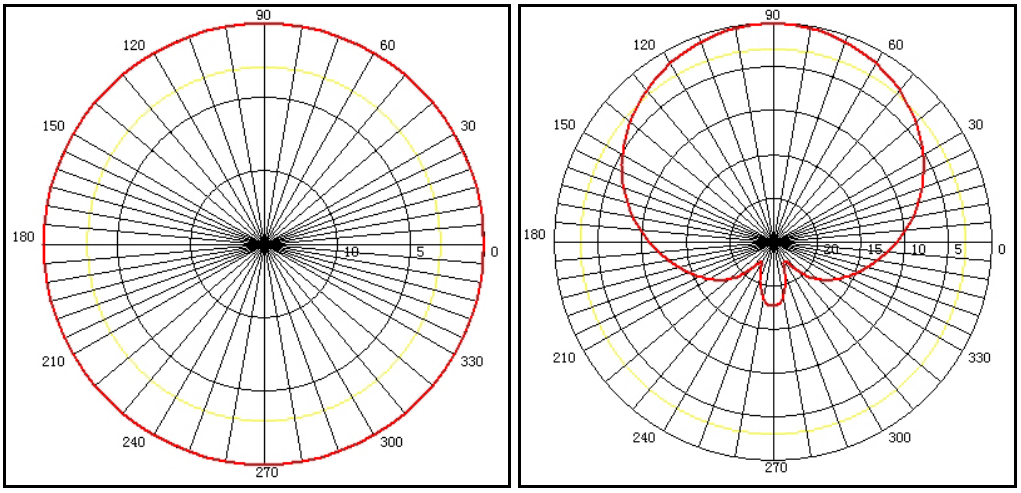

Figure 11.
These images give a bird's-eye view of how different antennas can generate signals in different patterns. The image on the left would be an example of an omni-direction antenna while the right image would target a certain sector between 60° and 120° (Images courtesy of Superpass Company Inc.).

A good example would be a flashlight, which does not shed light in all directions, but is aimed in a specific direction. The brightest area is that which is right in line with the flashlight, and diminishes as you move away from this centerline, as well as if you move further away from the light. Similarly, a wireless signal is strongest directly in front of the transmitter antenna and diminishes with distance, as well as with angle from its centerline. The transmitter's radiation pattern varies with the frequency being generated just as a flashlight would if it were more or less powerful. In this study distance was not an issue. All frequencies have a limit on the distance they can travel before the received power significantly diminish but signal strengths taken for this study were within a satisfactory range. Angle from the centerline was important though, and so it was necessary to manually redirect the transmitter once our recording location drifted too far from the its centerline, similar to the way you would redirect a flashlight to obtain the brightest light. Since Tim and I were walking the receiver equipment around and collecting data, my wife, Lisa, was kind enough to volunteer to help with redirecting the antenna. Therefore as Tim and I moved around, she would turn the antenna to point

directly at us, allowing all measurements to be taken in the center of the transmitter's beam. A set of Motorola walkie-talkies was used to help her in adjusting the transmitter when she could not see us.

3.5 Preparing the Collected Data

After I had collected my data I then needed to prepare it for analysis just as I did for my 16 grids. I began by downloading my 101 site locations from the handheld GPS unit. This was accomplished using the latest version of PC-GPS software, which resulted in a shapefile in geographic coordinates. The benefit of using a differential GPS unit is that data collected autonomously can then be corrected for increased accuracy. The National Geodetic Survey is continuously recording precise GPS satellite locations at various base stations across the country. Micro Corvallis claims their GPS unit to have an accuracy of 1 to 5m after correction. Visual inspection of the original uncorrected shapefile versus the corrected showed that some locations were significantly relocated. The following information reveals that most relocation was not extreme but a few outliers did exist (figure 12).

Maximum Difference:	16.6 meters
Minimum Difference:	0.5 m
Average Difference:	4.8 m
Median Difference:	3.8 m

Obtaining the highest possible degree of accuracy is critical when working with LiDAR data which is capable of measuring location at less than a meter in accuracy. The corrected shapefile containing all 101 sites was then projected to match the 16 grids. All additional information recorded at each location, i.e. signal strength, visual obstructions, etc., were entered into the attribute table of the shapefile.

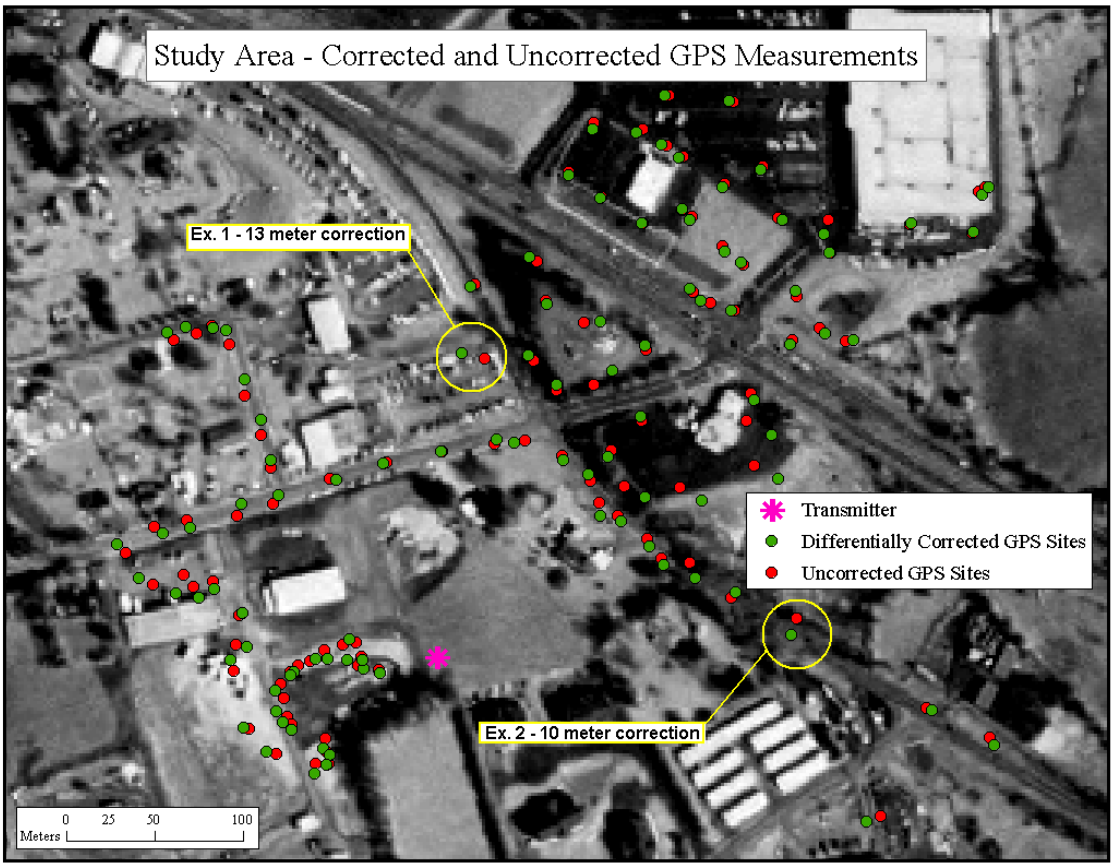

Figure 12.
Map illustrating the effects of using differential correction on autonomously collected GPS measurements.

3.6 LOS Thresholds

To finish preparing the data for analysis I needed to take the signal strength recordings collected for each site, which fell within a continuous range, and make them discrete. Each location had to be classified as either line-of-sight (LOS) or NLOS. Signal strength within a commshed is continuous. In my analysis, the GIS program predicts LOS at each of these 101 sites, not signal strengths, and therefore the collected field data needed to be discrete in order to compare the two. Signal strengths were measured at each site but obstacles in the path between the transmitter and receiver may have weakened this signal. Since LMDS signals have a predictable pattern in which they lose signal strength in an unobstructed path, known as path loss, the 'expected' signal strength could be calculated for each site based on its distance from transmitter. Therefore this expected strength for each site represented how strong the signal would be

if there were a clear path between the transmitter and the receiver (free space). A variety of components needed to be incorporated when expected signal strengths were calculated. These components included transmitter power, antenna gains, and receiver gains. The resulting equation is referred to as the Friis formula.

$$P_r = \frac{P_t \cdot G_t \cdot G_r}{L_i \cdot PL}$$

where, P_r is the received power, P_t is the transmitted power, G_t is the transmitter's antenna gain, G_r is the receiver's antenna gain, L_i is the implementation loss of the system, and PL is the free space path loss equal to $\left(\frac{4 \cdot \pi \cdot d}{\lambda}\right)^2$ where d is the distance between the transmitter and receiver and λ is the wavelength.

One method for determining expected signal strength is to choose one site where a signal strength measurement was recorded to become the reference site. This reference site needs to be representative of free space, relatively close to the transmitter, with a visually clear path to the transmitter. The estimated specifications for both the transmitter and the receiver (i.e. transmitter power, antenna gains, and receiver gains) indicated that signal strength at site #2 closely matched what the expected signal strength would be at that distance. This match indicated that this site's measured signal strength closely resembled the expected strength. The strength measurement and path distance for site #2 was then used to determine expected signal strengths for the remaining sites. The following formula was used to calculate these expected values.

$$P_r\,(dBm) = P_{ro}(dBm) + 10 \cdot \log_{10}\left(\frac{d_o}{d}\right)^2$$

where P_r is the received signal strength predicted at a location d meters from the transmitter and P_{ro} is the measured signal strength at the reference distance d_o meters from the transmitter.

Using reference values from site #2:

$$P_r\ (dBm) = -9.2\ dBm + 10 \cdot \log_{10}\left(\frac{49.6\ m}{d}\right)^2$$

The difference in signal strength values can be extremely large and so computations are simplified and precision maintained by working in log format. These logarithm values are measured in decibels (dB) where gains or losses are represented or dBm when the signal is referenced to 1mW. (Weisman, 2000).

After expected values were determined, measured signal strength needed to be subtracted (in dB) from these expected values to reveal the difference between the two. If the path between the transmitter and any given location were clear, then we would assume that the measured signal strength would be close to the expected strength. Signal paths that were blocked would produce a much lower strength than expected because reflected and diffracted paths suffer greater loss than LOS. These sites would have large differences between expected and measured signal strength. In between these two extremes lies a gray area representing partially blocked signals that fall along a continuum of measured versus expected signal strength differences.

The final step would be to determine a threshold that would determine the difference between LOS and NLOS paths. Put another way, if the difference between the expected and measured signal strength was greater than a certain amount, we would consider that path not to have radio wave LOS because it may be blocked by something in the environment (i.e. vegetation, buildings, etc.). Previous work by Rose (2001) has suggested a -3dB to -6dB difference to be an acceptable threshold level to classify signal strength into LOS or NLOS. Plotting the measured versus expected signal strength as a log function did not reveal an obvious breaking point but that was not expected since a portion of the sites were partially blocked (figure 13). I chose a variety of threshold ranges to determine if this decision may have a strong influence on my overall results. I used -3 dB, -6 dB, -9 dB, and -12 dB thresholds to classify signal strength into LOS or NLOS. In addition, I used the visual observations on LOS/NLOS as a fifth threshold level. While recording data in the field I had noted whether the path between each site and the antenna was partially or completely blocked or whether it was clear. If I used these visual observations as a way to classify my sites I could also test to see how well

they did in predicting signal strength. Can an accurate commshed be predicted just by saying that sites in view from the transmitter have LOS and those not seen from the transmitter will not? Although this would be an impractical method to determine a commshed I felt that the results might reveal some useful information. I chose not to include any sites that were noted as partially blocked and simply used sites that were noted as completely visible or completely blocked. See Appendix C.

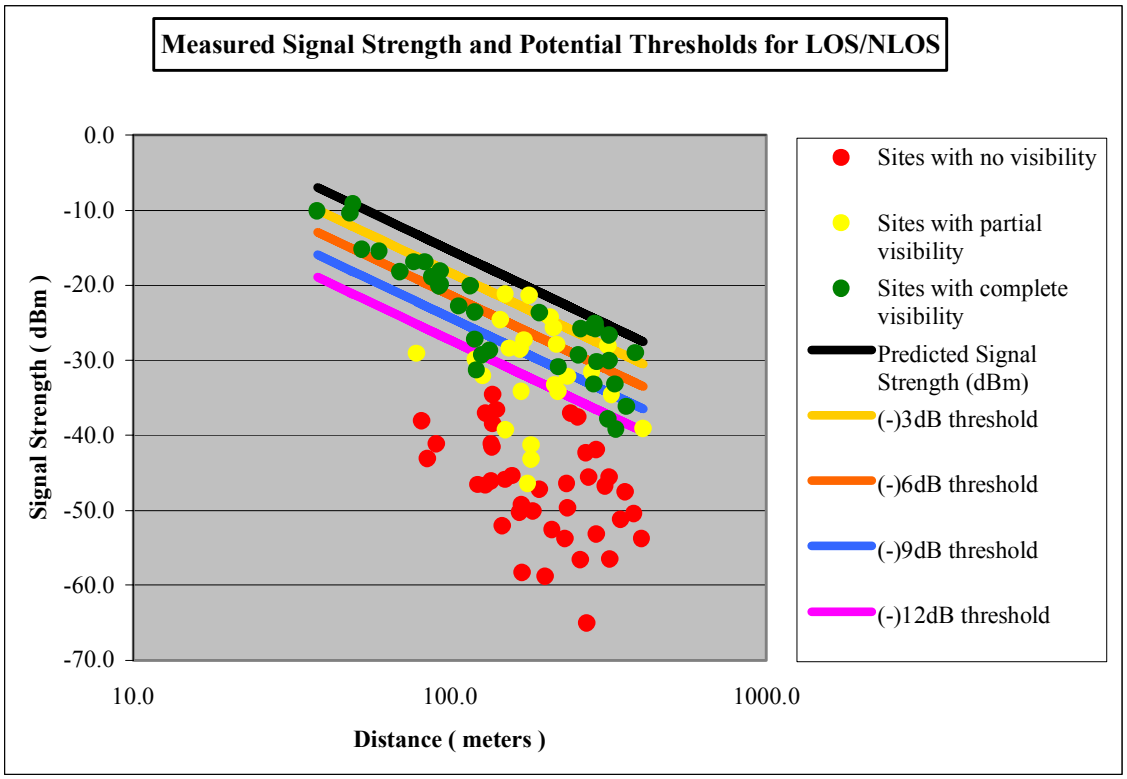

Figure 13.
This chart shows the distribution of signal strengths in addition to the predicted signal strength (black). Each of the four potential threshold classifications is shown below the predicted signal strength line. The fifth threshold classification was based whether these sites were visible from the antenna (only green and red points).

Using five different thresholds resulted in five separate classifications of all sites. The following summary indicates the distribution of sites for each these classes.

Classification	LOS Sites	NLOS Sites	Totals
-3dB Threshold	14	87	101
-6dB Threshold	30	71	101
-9dB Threshold	40	61	101
-12dB Threshold	49	52	101
Visibility Threshold	37	40	77

Each of these results would be used as the 'true' commshed during analysis. Therefore the study will not only test predicted signal strength based on different resolutions but will also see if threshold decisions can be influential when classifying signal strength.

Chapter 4: Analysis and Results

4.1 Introduction

Analysis began with the 16 prepared grids and one shapefile containing all 101 sites where field data was collected. The first step of the analysis required creating a predicted commshed using each of these grids as the elevation model. Each predicted commshed assigned either LOS or NLOS to each site. The second step of the analysis would statistically compare each of the 16 predicted commsheds against the 'true' commshed to provide an estimate as to how well each resolution supported the prediction. A third step compared all predicted commsheds among themselves to determine any significant differences between certain resolutions. A particular resolution may accurately predict the 'true' commshed, but it may be significantly better at doing so when compared to its neighboring resolutions. A fourth and final step was to determine if the five different threshold levels used to classify our 'true' commshed had any influence on the results. GETWEBS, Geographic-Engineering Tool for Wireless: Evaluation of Broadband Systems (Carstensen, 2001), is a GIS program used in this study that was designed specifically for wireless network designs and layouts. This program was created specifically for the wireless industry and allows the user to enter a range of information from equipment costs to detailed transmitter specifications (figure 14). GETWEBS also has been designed to incorporate a signal's fresnel zone clearance so that the GIS program's modeling capabilities will more closely resemble the true characteristics of radio wave propagation. As mentioned previously, the fresnel zone is an area surrounding the LOS path between two points and is important in calculating signal strength. From this point onward LOS should be interpreted as clearing the first fresnel zone.

4.2 Predicted Commsheds

The first step required creating a predicted commshed for each of the 16 grids. Once the site shapefile was loaded into GETWEBS, an antenna file was created, to hold all information pertaining to the transmitter specifications. The goal was to model as closely as possible all information in the GETWEBS program to match the transmitter

setup used in Wytheville. The location assigned to this antenna file matched to true location of the transmitter when field data was collected. The following information was entered into the antenna file that would be used by the GETWEBS program.

Antenna height: 1 m

Predicted range of commshed: 450 m

Left azimuth: 200 degrees (north being 0 degrees)

Right azimuth: 120 degrees (north being 0 degrees)

Vertical Range: 0 to –10 degrees

Radio Wave Frequency: 28 GHz

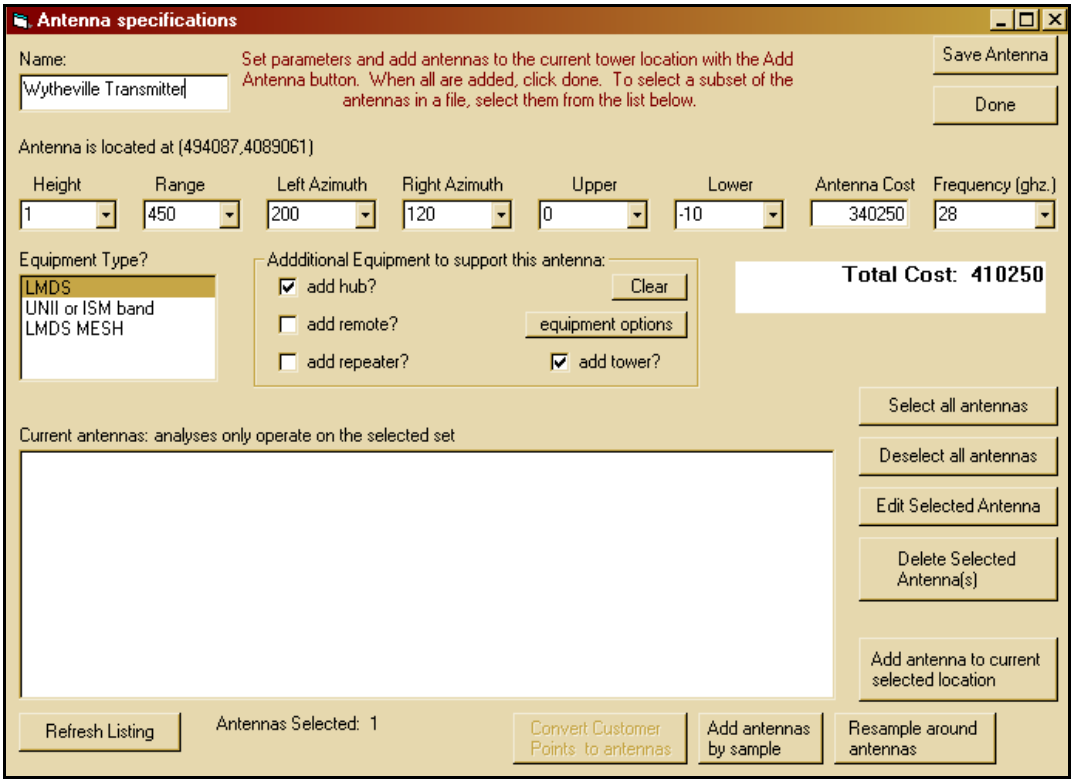

Figure 14.
GETWEBS software gives the user a great deal of control
in setting up the antenna specifications.

The height of the antenna was set at 1m to match the height of the antenna during actual data collection. The predicted commshed only needed to cover an area that held the 101

sites and therefore the range of the antenna was set to cover the most distant sample point. LMDS generated signals can propagate much further, but to reduce computer-processing time the program only needed to calculate LOS for areas containing the 101 sites. Sector azimuths were set for the same reason and the vertical range was determined by equipment design. The 'true' commshed frequency of 27.810 GHz was modeled in the program using 28 GHz. After all information had been entered, the antenna file was a close representation.

Once the antenna file was setup, the program needed a grid in order to compute the commshed. In order to calculate a commshed two pieces of information are needed: a point location representing where the transmitter was setup (antenna file) and a raster layer with cell values containing elevation data (16 grids). Therefore the 1m LiDAR grid was loaded to create the first of 16 predicted commsheds. When calculating a commshed, standard GIS programs simply highlight all areas that have LOS with the transmitter location. One added benefit of the GETWEBS program is that it can also look at individual sample points and decide on LOS or NLOS. It not only provides a new grid that shows all LOS areas, but it can take another shapefile of points and tell the user whether or not each point had LOS. This added benefit of the software provided the information at each of the sites that would be used to determine the accuracy of each predicted commshed. Once the location shapefile showing all sample sites was loaded, the program could quickly assign LOS or NLOS to each site. Once the initial 1m LiDAR grid was imported into GETWEBS, a predicted commshed was calculated, resulting in both a commshed grid highlighting areas having LOS as well as a Microsoft Excel file listing which of the 101 locations had LOS with the antenna. This procedure was performed on each of the 16 grids resulting in 16 predicted commsheds as well as 16 MS Excel files indicating sites having LOS with the transmitter (example of the 5m grid in figure 15, all results are shown in Appendix D).

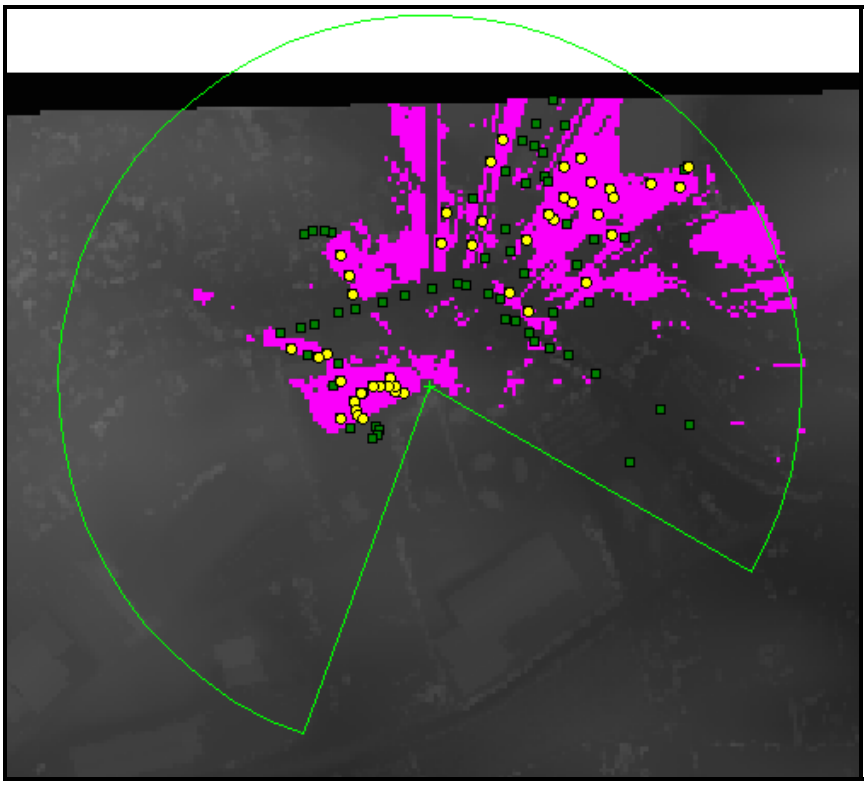

Figure 15.
This predicted commshed shows the output of the GETWEBS program on a 5m resolution LiDAR created grid. Purple indicates areas that have LOS with the antenna. Points represent the 101 sites with yellow symbols having predicted LOS and green symbols not having LOS.

4.3 Error Matrices

GETWEBS provided information to be assessed for accuracy on all 101 sites for all 16 grids. To determine how accurate each commshed was in its own prediction it needed to be compared to each of the five 'true' commsheds. An analogous situation occurs often in the field of remote sensing in determining the success of image classification. Remote sensing analysts will classify an accurate 'reference' map based on a predefined set of categories and then test the newly classified map to determine the accuracy of the classification process. Congalton (1981) developed a method using an error matrix to test this success. "An error matrix is a square array of numbers set out in rows and columns which expresses the number of cells assigned as a particular land cover type relative to the actual cover type as verified in the field" (Congalton 1981, p.4). An error matrix looks at the resulting classified image, compares it to the reference image being classified, and provides the user with an overall accuracy. This accuracy indicates

the success of the classification process. This principle of using error matrices to determine accuracy in comparing two images can be applied to this study. In this study, the five 'true' commsheds are considered the reference images that need to be classified, or in this case, predicted. The GETWEBS program uses various resolution grids to predict commsheds and provides the classification process. The error matrix can then be used to compare the 'true' commsheds against each of the 16 predicted commsheds to determine the success of the prediction.

An error matrix can be used to test either site-specific or non site-specific accuracy. Non site-specific accuracy looks at overall percentages and does not consider location in the classification process. This study utilized site-specific accuracy since it was interested in testing predicted commsheds at specific locations that had been measured using GPS methods. Campbell states that site-specific accuracy is "based upon the detailed assessment of agreement between two maps at specific locations" (Campbell, 2002 p.389). Signal strength measurements taken of the 'true' commshed, after converting them from continuous to discrete, were of categorical nature, either LOS or NLOS, and fell within each category without ambiguity. Each site was classified five different ways based on each of the five threshold levels. See Appendix C. By using categorical data, the need to test for normality is eliminated (Congalton, 1981). There is still little agreement on a correct sampling scheme and total number of samples required in collected data used in error matrix analysis. Congalton suggests choosing a number that "maximizes information with the minimum amount of work" (1981, p.8).

Using Campbell (2002) as a reference, I was able to construct an error matrix for each predicted commshed. The error matrix was a simple 2X2 array, of which, one axis would be the 'true' commshed and the other the predicted commshed. Each side had a LOS and NLOS category. This matrix created 4 categories: correct LOS, correct NLOS, incorrect LOS when NLOS, incorrect NLOS when LOS. If the 'true' commshed indicated LOS, as did the predicted commshed, then this counted as a correct prediction. This was the same for correctly predicted NLOS. An "incorrect yes when no" meant that the predicted commshed had LOS when the 'true' commshed was NLOS and vice versus for the 'incorrect no when yes' category. This site-by-site comparison provided the values for each of the four categories in the matrix (figure 16).

	1m-IN	1m-OUT						Total Samples	101
In	24	7	31					Total Correctly Classified	78
Out	16	54	70					Percentage Correct	77.23%
	40	61	78						
	Expected by Chance								
	1240	1891						'Observed Correct'	0.7723
	2800	4270						'Expected Correct'	0.5401
		Sum of Diag.	5510					"KHAT"	0.5048
		Total Sum	10201						50.48%

Figure 16.
This error matrix is one of many comparisons done
between predicted and 'true' commsheds.

4.4 Determining Accuracy

Using each error matrix to determine the accuracy of the predicted commsheds was accomplished in two steps. First, the individual significance and accuracy of each commshed needed to be determined. A second step then compared each commshed to all other commsheds to determine significant differences among them. Both steps resulted in the following information for each of the five threshold levels of classification:

- Error matrix for all 16 grids
- Overall accuracy for all 16 grids
- Khat scores for all 16 grids
- Significance of Khat scores for all 16 grids
- Significance when comparing all 16 grids to one another

The following sections detail the methods used in each step of the analysis and the resulting outcomes. The reader should understand that this entire procedure was performed five different times using each threshold classification. Original signal strength measurements were classified using five different threshold levels resulting in five 'true' commsheds. Therefore 16 predicted commsheds created using various resolutions were compared against 5 different 'true' commsheds. For the following explanations, each of these five different commsheds will be referred to as the 'true' commshed for simplicity.

4.5 Overall Accuracy

Once comparing all grids against the 'true' commshed created 16 error matrices, a more powerful analysis could be performed. To give a general idea on how well each prediction did, its overall accuracy (percent correct) could be calculated by dividing all correctly predicted sites by the total number of sites. Using the example in Figure 16, 78 out of 101 sites were correctly predicted resulting in an overall accuracy of 77.23%. This would indicate that the 1m resolution did fairly well in predicting the correct commshed. Figure 17 shows the overall accuracy of all 16 grids for each of the five 'true' commshed classifications.

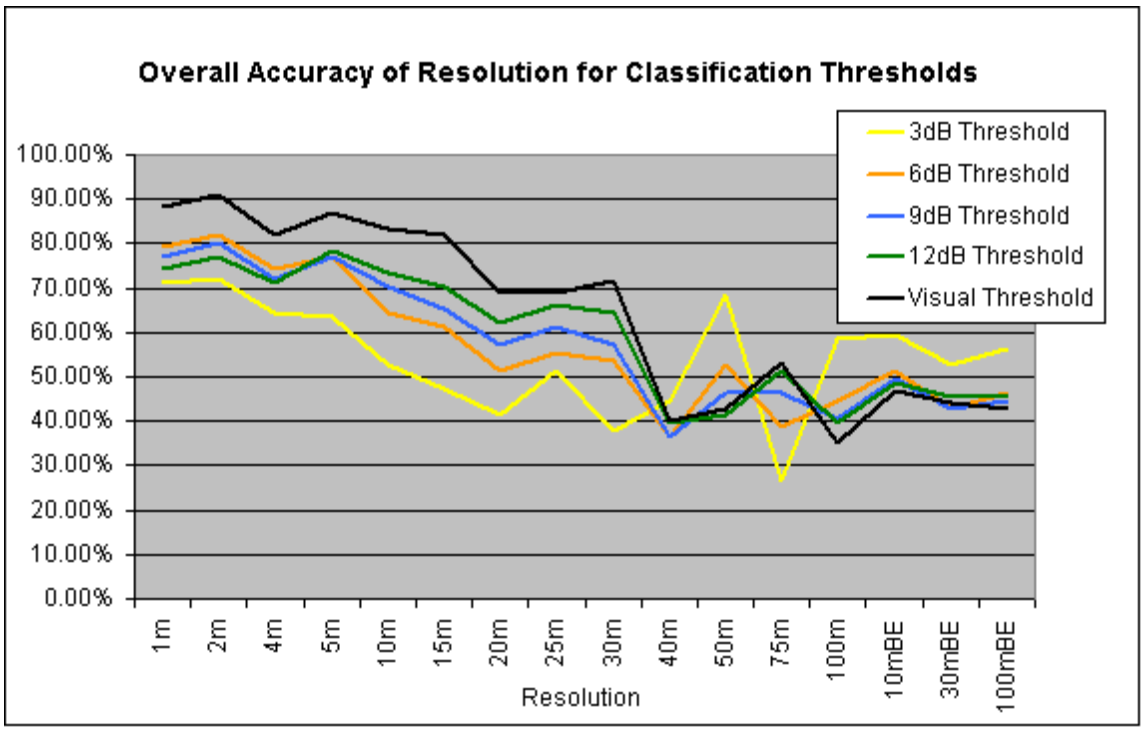

Figure 17.
This chart shows the overall accuracy for each of the five threshold classifications across each of the 16 resolutions.

Accuracy appeared to have a direct correlation with resolution. Overall accuracy was high when grid resolution was also high while decreasing in accuracy with lower resolutions. The visibility threshold had the highest accuracy for higher LiDAR resolutions but did not differ from other thresholds at lower resolutions. The –3dB

threshold had the lowest accuracy at higher resolutions but higher accuracy at lower resolutions, especially the three bare-earth grids. All other thresholds were relatively similar in their accuracy at lower resolutions. In general, all thresholds followed a trend from high to low resolution with the –3dB threshold differing the most.

4.6 Khat Scores and Significance

A stronger statistic offered by the matrix is the Kappa analysis, which can be approximated by the Khat score. Overall accuracy is useful but the Khat score eliminates any part of this accuracy obtained by chance agreement. Some agreement between commsheds can exist simply by chance and should not be attributed to the success of the prediction. The Khat score adjusts the previously described overall accuracy by removing this chance agreement (Campbell 2002). Khat scores can range from +1 to –1 but can also be shown as percentages for comparisons to overall accuracy. Congalton (1999) states that 'a value greater than 0.80 (i.e., 80%) represents strong agreement; a value between 0.40 and 0.80 (i.e., 40-80%) represents moderate agreement; and a value below 0.40 (i.e., 40%) represents poor agreement' (p. 51). Figure 18 shows the Khat scores of all 16 grids for each of the five 'true' commshed classifications. Not all grids were successful and some dropped below 0% in accuracy once chance agreement was removed. Khat values at or below 0% indicate the grid did not predict the correct commshed any better than if it were randomly chosen. Khat score followed a trend similar to overall accuracy. Higher resolutions were more accurate than lower resolutions. Once again, the visibility threshold provided more accuracy at higher resolutions while not differing from other thresholds at lower resolutions. Lower resolutions did not show much difference between threshold classes but dropped close to or below 0% indicating that these resolutions could not predict a commshed any better than if it were randomly chosen. The –3dB threshold was most successful in bare-earth resolutions but only had a Khat score from 7-10%. This low Khat score for the –3dB threshold can possibly be explained by simple fluctuations in the equipment causing overall signal loss. Often times wireless equipment used in radio wave propagation has inherent fluctuates that can cause measured signal strength to range +/- 3 dB around the expected signal strength. Using just equipment fluctuations as a threshold would not

provide an accurate prediction because there is no allowance for addition differences between expected and measured signal strength.

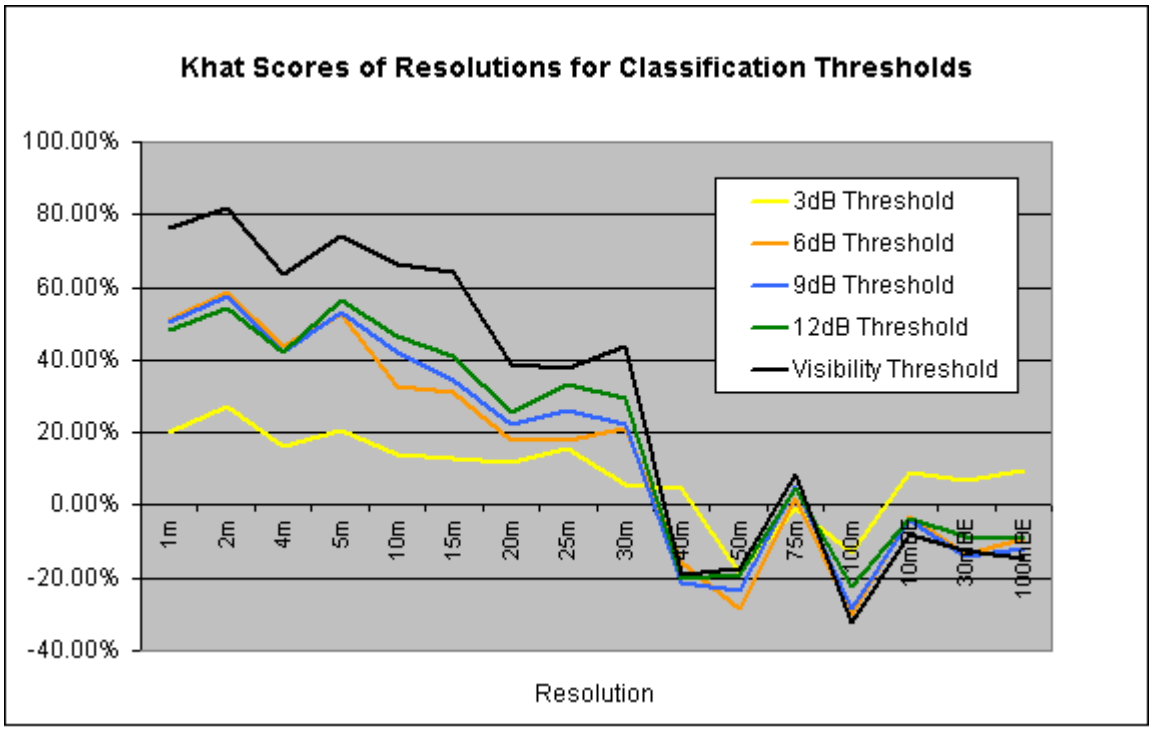

Figure. 18
This chart shows Khat scores for the five threshold classifications across each of the 16 resolutions.

One noticeable difference between overall accuracy and Khat scores can be seen in higher resolutions. Higher resolutions that had high overall accuracy did not decrease equally across thresholds when chance agreement was removed. The visibility threshold remained high across both while the other threshold levels dropped in accuracy. The visibility threshold started with overall accuracy between 80-90% and after removing chance agreement had accuracy between 60-80% while the –3dB threshold started with approximately 60-70% in overall accuracy but dropped to approximately 20% in Khat scores. Figure 19 illustrates this difference. The visibility threshold exhibited much less change than the –3dB threshold as indicated by the red lines.

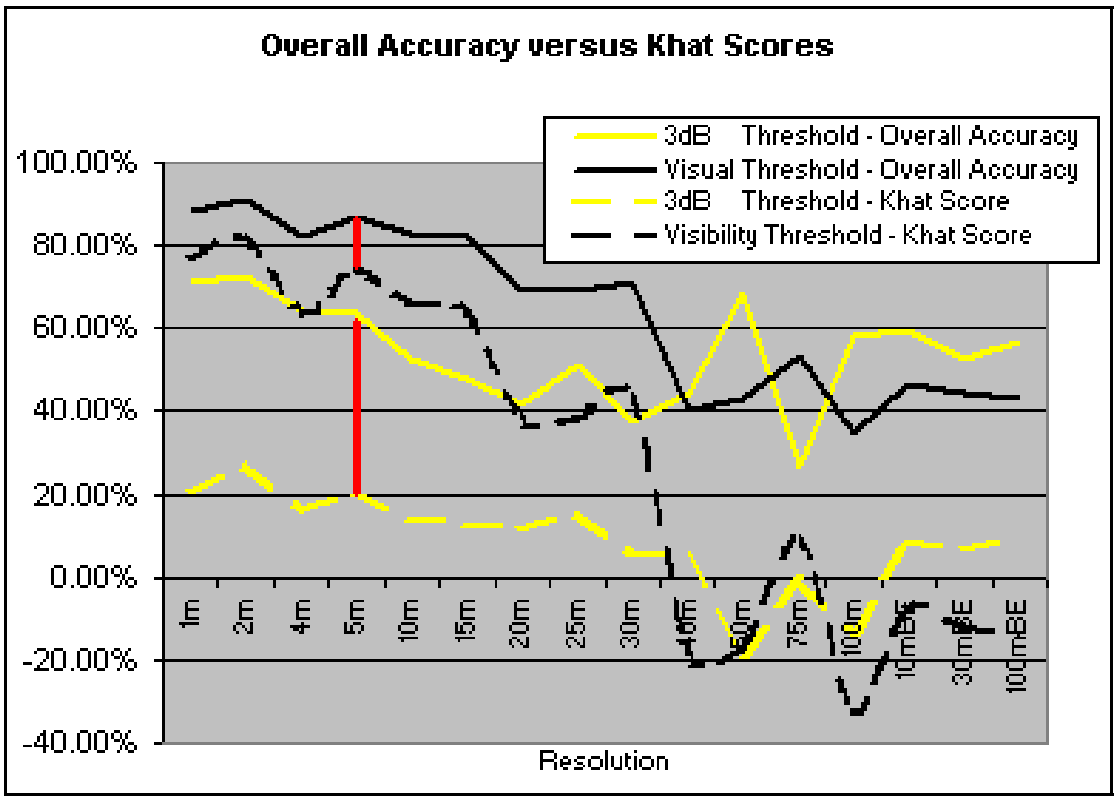

Figure 19.
This figure shows that the removal of chance agreement
was not equal for all threshold levels.

Looking at the error matrices for both threshold classifications seen in above, there appears to be noticeable differences in their observed correct values when compared to their expected correct values (chance agreement). These observed and expected values are used in computing Khat scores. A larger difference between the two results in higher Khat scores. If a grid has a high overall accuracy but a low chance agreement, then less accuracy will be subtracted from the overall accuracy when computing Khat scores. If chance agreement is high, more will be removed from overall accuracy. See Appendix E for a complete breakdown of overall accuracy and Khat scores for all grids. Although both the visibility and the –3dB thresholds had high overall accuracy at higher resolution, the visibility has less chance agreement subtracted resulting in a higher Khat score.

Figure 18 above also shows a significant drop in Khat values between the 30m and 40m resolutions. Resolutions higher than 30m show a gradual change in Khat scores but then decreases drastically once it approaches 40m. Comparing error matrices

between the 30m and 40m resolutions shows a decrease in overall accuracy with an increase in expected error. A smaller difference between predicted accuracy and chance agreement results in a lower Khat score, explaining this situation. Looking at the two different commshed images for the 30m and 40m resolutions also helps to illustrate this significant change in Khat score (see Figure 20). The area indicated in blue contains sites having LOS based on the 'true' commsheds. The 30m-resolution image on the left shows these sites being predicted as having LOS while the 40m-resolution image on the right does not. All resolutions higher than 30m also predicted LOS for these points while lower resolution did not. This large grouping of sites that are inaccurately predicted in resolutions 30m and below is one explanation for the significant drop in Khat scores.

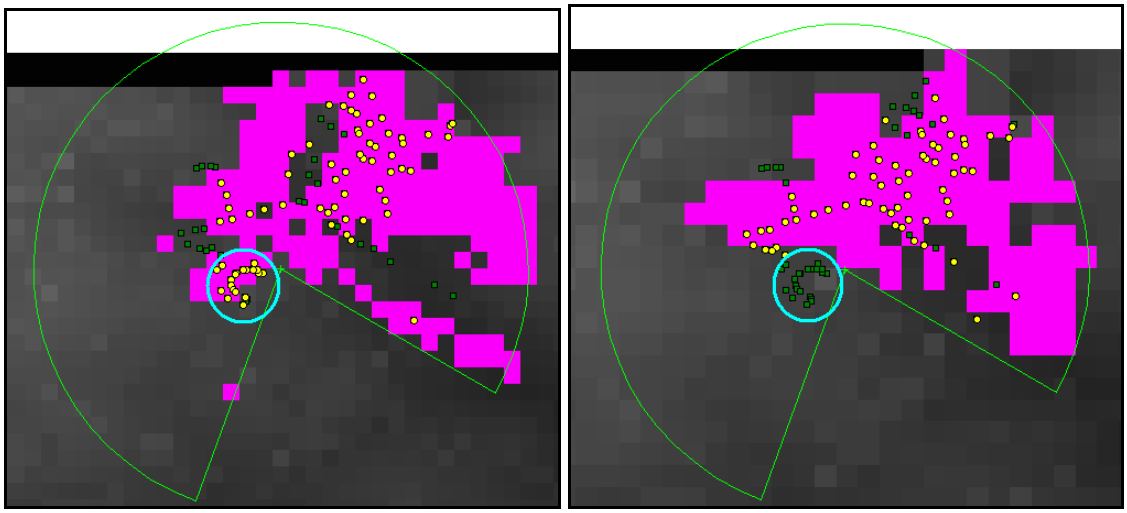

Figure 20.
These two predicted commsheds show a large grouping of sites that have LOS in the 30m-resolution image on the left but do not have LOS on the 40m-resolution image on the right.

Khat scores for each predicted commshed help to determine how well each did in its prediction when compared to chance agreement. It is also possible to compute a Z test for each of these predicted commsheds to determine if this difference between predicted and chance is significant. This requires calculating a variance, which then is used to determine a confidence interval around the Khat score. A resulting Z score greater than or equal to the critical value of 1.96 for a .05 alpha confidence level is considered significantly better than chance when the degrees of freedom are greater than 30. Although measurements were taken at 101 sites, the number of grid cells in which these

101 sites fell fluctuated depending on grid resolution size. This total number of cells was greater than 30 for 13 out of the 16 grids. The 101 sites fell within fewer than 30 cells for the 75m LiDAR grid, the 100m LiDAR grid, and the 100m bare-earth DEM resulting in an increase in the critical value for significance. The 75m LiDAR grid had 26 cells in which all sites were located increasing the critical value for significance to 2.06. Critical values for the 100m LiDAR grid having 19 cells and the 100m bare-earth DEM having 21 cells resulting in critical values of 2.09 and 2.08 respectively. Each of these 3 grids had extremely low Khat scores to begin with and this slight increase in critical values had no influence on their resulting success. See Appendix F for a complete list of individual significance tests. Figure 21 shows how well each resolution faired across threshold classifications. It is difficult to make any direct statements about the distribution of significance but there does appear to be a trend from –3dB toward the visibility threshold as indicated in yellow.

	3 dB	6 dB	9 dB	12 dB	Visibility
1m	NOT SIG	SIG	SIG	SIG	SIG
2m	SIG	SIG	SIG	SIG	SIG
4m	NOT SIG	SIG	SIG	SIG	SIG
5m	NOT SIG	SIG	SIG	SIG	SIG
10m	NOT SIG	SIG	SIG	SIG	SIG
15m	NOT SIG	SIG	SIG	SIG	SIG
20m	NOT SIG	NOT SIG	NOT SIG	SIG	SIG
25m	NOT SIG	NOT SIG	SIG	SIG	SIG
30m	NOT SIG	NOT SIG	NOT SIG	SIG	SIG
40m	NOT SIG	NOT SIG	NOT SIG	NOT SIG	NOT SIG
50m	NOT SIG	NOT SIG	NOT SIG	NOT SIG	NOT SIG
75m	NOT SIG	NOT SIG	NOT SIG	NOT SIG	NOT SIG
100m	NOT SIG	NOT SIG	NOT SIG	NOT SIG	NOT SIG
10mBE	NOT SIG	NOT SIG	NOT SIG	NOT SIG	NOT SIG
30mBE	NOT SIG	NOT SIG	NOT SIG	NOT SIG	NOT SIG
100mBE	NOT SIG	NOT SIG	NOT SIG	NOT SIG	NOT SIG

Figure 21.
Individual significance for each resolution across all five threshold classifications.

As the threshold becomes larger it becomes less restrictive on which sites it will classify as LOS. In other words, larger thresholds allow sites having a larger difference between

their measured signal strength compared to their predicted to be accepted as LOS. The –3dB threshold was very stringent, allowing only the 2m grid to be significant over chance agreement. Thresholds of –6dB and –9dB appeared less stringent and similar except for a disagreement over the 25m resolution. The -12dB and visibility thresholds had the exact same significant grids indicating that the commshed predictions are equivalent in accuracy. These results would indicate that using a –3dB threshold requires a very high-resolution grid to obtain an accurate prediction over chance. Progressively less stringent threshold levels provide more significantly accurate predictions at less detailed resolutions.

4.7 Within Threshold Comparisons

Individual significance only compares each predicted commshed against chance agreement. This study also compared each predicted commshed against all other commsheds within each of the five threshold classifications. Determining significant differences simply meant looking at the confidence intervals for two predictions being compared and no overlap was considered significant. Similar to individual significance, Z scores were compared against the critical value of 1.96. This resulted in a total of five different charts based on each of the threshold classifications. See Appendix G. Results followed a trend similar to that of individual significance. Figure 22 shows the results of the among resolution comparisons for the –3dB classification. Diagonal cells in gray indicate commshed comparisons of the same resolution and therefore hold no difference. Green cells highlight comparisons that were shown to be significantly different while cells in orange indicate comparisons that are not significantly different. For the –3dB resolution there is almost no difference among any of the resolutions. The 50m resolution is significantly different from many higher resolutions but only because of its extremely poor Khat score. This helps to show that significance does not mean accuracy and may indicate significantly poorer predictions as opposed to successful ones. It is therefore necessary to use this comparison along with individual significance to differentiate between successful and poor resolutions.

	1m	2m	4m	5m	10m	15m	20m	25m	30m	40m	50m	75m	100m	10mBE	30mBE	100mBE
1m	NOT															
2m	NOT	NOT														
4m	NOT	NOT	NOT													
5m	NOT	NOT	NOT	NOT												
10m	NOT	NOT	NOT	NOT	NOT											
15m	NOT	NOT	NOT	NOT	NOT	NOT										
20m	NOT	NOT	NOT	NOT	NOT	NOT	NOT									
25m	NOT	NOT	NOT	NOT	NOT	NOT	NOT	NOT								
30m	NOT	NOT	NOT	NOT	NOT	NOT	NOT	NOT	NOT							
40m	NOT	NOT	NOT	NOT	NOT	NOT	NOT	NOT	NOT	NOT						
50m	SIG	SIG	SIG	SIG	SIG	SIG	NOT	SIG	NOT	NOT	NOT					
75m	NOT	NOT	NOT	NOT	NOT	NOT	NOT	NOT	NOT	NOT	NOT	NOT				
100m	NOT	SIG	NOT	NOT	NOT	NOT	NOT	NOT	NOT	NOT	NOT	NOT	NOT			
10mBE	NOT	NOT	NOT	NOT	NOT	NOT	NOT	NOT	NOT	NOT	NOT	NOT	NOT	NOT		
30mBE	NOT	NOT	NOT	NOT	NOT	NOT	NOT	NOT	NOT	NOT	NOT	NOT	NOT	NOT	NOT	
100mBE	NOT	NOT	NOT	NOT	NOT	NOT	NOT	NOT	NOT	NOT	NOT	NOT	NOT	NOT	NOT	NOT

Figure 22.
This chart shows significance between all grids using the –3dB threshold level.

The other four threshold levels were not as restrictive in their comparisons. It is difficult to compare such large charts against one another but visual inspection reveals some similar groupings among the remaining four within group comparisons. In general, resolutions from 1m to 15m gave significant prediction success and were not significantly different from one another (figure 23). Therefore using a 1m resolution would provide the same amount of accuracy as using a 15m resolution. Similarly, resolutions of 75m and 100m, including all three bare-earth grids showed no significant difference among themselves. All resolutions in this latter grouping had neither individual significance nor significant difference among them, indicating that they all performed equally as poorly in their predications.

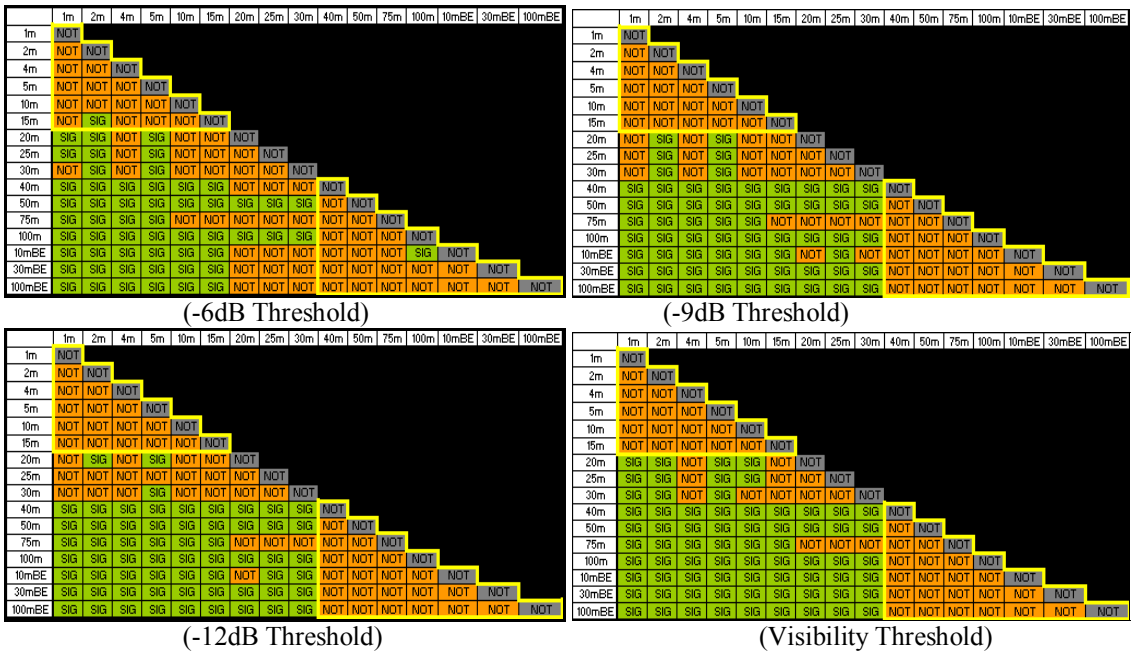

Figure 23.
The remaining four threshold comparisons charts reveal groupings of resolutions that are not significantly different among from one another (highlighted in yellow).

Higher threshold levels of -12dB and visibility show more within threshold differences than the lower threshold levels of -6dB and –9dB indicated by more significant differences between neighboring resolutions. This can be explained by looking back at Figure 18. More change in Khat scores when comparing neighboring resolutions would indicate more differences between them. In other words, the more steep the decline in Khat values, the more chance for difference between neighboring grids. The visibility threshold had the highest change in Khat scores, with a range of 81% to –32%, a difference of over 100. The –3dB threshold, had the smallest difference in Khat scores ranging from 27% to –13%, a difference of approximately 40. The visibility had much more within threshold significant differences while the –3dB threshold had almost none. Therefore the more change in Khat scores, the more chance there is for significant difference among the grids.

Discussion and Conclusion

5.1 Conclusion

This study set out to answer three questions.

- Are bare-earth DEMs just as accurate at predicting LOS in 28GHz radio frequencies when compared to LiDAR imagery, or does LiDAR's incorporated surface features provide enough added information to render a more accurate prediction?
- Are there any differences within varying resolutions of LiDAR? Looking strictly at LiDAR, does a more detailed resolution provide more accuracy over a less detailed one?
- Finally, does the classification process of changing continuous signal strengths into discrete LOS or NLOS classes have any influence on testing the accuracy of a predicted commshed?

The results indicate significant differences between bare-earth DEMs and LiDAR, but are dependent on the 'true' commshed classification. Stringent classifications that allow a –3dB difference from the predicted strength when determining LOS indicate no difference between bare-earth DEMs and LiDAR. All bare-earth DEMs as well as all LiDAR resolutions, except the 2m LiDAR grid, had equally poor predictions and were no more accurate than a randomly chosen prediction. When thresholds were increased to –6dB and –9dB, more differences appeared between LiDAR and bare-earth grids. LiDAR resolutions of 15m and higher supported significant predictions over chance while lower resolutions, including all bare-earth DEMs, still could not provide an accurate prediction. In general, there were no significant differences between the 1m and 15m LiDAR resolutions indicating that one grid would be just as accurate as another would. If thresholds were increased once again to include –12dB or LOS visibility, the total number of accurate predictions increased once again. LiDAR resolutions between 1m and 30m became significantly more accurate than a chance prediction while lower resolution LiDAR grids and bare-earth DEMs still could not provide an accurate

prediction. At these less stringent thresholds there was still no differences between the 1m and 30m resolutions implying one to be as good as the another.

Therefore the importance of determining threshold levels is critical in finding a resolution that can produce accurate predictions. Bare-earth DEMs could not produce an accurate prediction regardless of threshold levels nor could LiDAR resolutions below 40m. The most stringent threshold classification indicated the only useful resolution to be the 2m LiDAR grid. A stringent threshold range of 3dB closely reflects inherent fluctuations in the wireless equipment and is not typically used in the field to determine an acceptable level for LOS. Increasing the threshold level to a range of 6dB or 9dB indicates that only high resolution LiDAR can provide an accurate prediction while lower resolutions still cannot provide that needed accuracy. An abnormally large threshold range of 12dB only increases the number of LiDAR resolutions that supported an accurate prediction. Finally, there appears to be no difference among accurate predictions, that is, one prediction is just as accurate when compared to other significant predictions.

The results of this study suggest using a 15m LiDAR grid to obtain a significant level of accuracy for modeling LMDS frequency radio wave propagation. Higher resolution LiDAR grids do not provide any additional accuracy. The cost to obtain LiDAR can be expensive and is partially dependent on the desired detail. It would be more cost effective to obtain the least amount of detail for the same amount of accuracy. There is little point in spending more for a 1m or 2m LiDAR grid when a 15m grid can provide the same accuracy. This study also reveals that bare-earth DEMs are a poor alternative to LiDAR when modeling LOS characteristics seen in LMDS frequencies. These results are limited to environments resembling the one use in this study. Other geographic locations that have less relief and less vegetation may show more support for bare-earth DEMs.

5.2 Addressing Error

It is important to address any potential sources of error that may have been encountered in this study. Error, which is inherent in any study, was considered and minimized. Two possible sources of error that seem the most significant in this study

include seasonal differences when comparing maps/images and equipment measurement limitations. This study used a technique, well known in the remote sensing industry, of comparing images to find difference between them. Remote sensing measurements, such as LiDAR imagery, record the earth's surface at an exact moment in time. Seasonal differences such as leaf cover changes on deciduous plants, can have an influence when comparing two images recorded at different times of the year and may or may not be desired by the analyst. LiDAR imagery used in this study was recorded in mid-September while field data collected on the 'true' commshed in Wytheville was recorded in early November. Although this is only a 6-week seasonal difference, it should be noted. Since almost any feature in the environment including leaves can influence higher frequency radio waves, it is important to address this discrepancy. Any differences could therefore influence the accuracy at specific sites that were measured behind deciduous vegetation and should be considered in future studies. Secondly, restrictions on equipment used in a particular study can have an influence on the results. For example, a GPS unit is only capable of measuring location to a certain degree of accuracy. More expensive units provide the user with more accuracy. Therefore the user needs equipment that will provide the accuracy required for the study. This study dealt with LiDAR data claiming accuracy of 1 meter while the GPS unit used in this study claims to have accuracy between 1 and 5 meters after being corrected. It is important to understand that collected data is often a representation of the true environment but always contains some portion of error. All gathered data holds some degree of error determined by restrictions on the measurement equipment and results can only be as good as the methods and equipment used. The results from this study also suggested one additional factor to consider when dealing with sampling methods and grid analysis. Sample sites measured within a small geographic area may all fall within one grid cell depending on resolution. Although each sample represents a different site they may not be considered different samples when used in grid analysis. This study handled this issue by increasing the critical value for significance tests but can be avoided in future work.

5.3 Future Work

The results of this study indicate a need for further work in the area of signal strength modeling. The results indicate that there are significant differences among the resolutions tested but were highly dependent on the threshold level used. More stringent thresholds were very limiting on which resolutions were accurate in their predictions while less restrictive thresholds provided an increase in accurate predictions. This indicates that the classification process of converting continuous signal strength into categorical LOS or NLOS had a large impact. It may be useful to design a program that can model signal strength as opposed to simply highlighting areas having LOS. If this program could provide a predicted signal strength at each site, it would be more accurate to simply compare modeled signal strength against field measured signal strength and avoid any conversion of data into LOS or NLOS. This would eliminate generalizing the data and allow the user to work with raw signal strengths measurements. Also, work done by Baldassaro (2001) indicates that it is important to incorporate signal diffraction while modeling wave propagation. Her study shows that determining signal strength simply by path loss is not as accurate as including the wave's ability to bend around objects in the environment. Future modeling tools may also look to include more characteristics of wave propagation. This study has shown that elevation data needs to include surface features to provide an accurate prediction when modeling higher frequencies. It has also shown that work is needed in creating a more powerful GIS tool, which can model radio wave signals that have LOS properties but are not true LOS.

Works Cited

Baldassaro, Paige. "RF and GIS: Field Strength Prediction for Frequencies between 900 MHz and 28 GHz." MS thesis in Geography – Virginia Tech, 2001.

Campbell, James. *Introduction to Remote Sensing.* 3rd ed. New York: Guilford Press, 2002.

Carstensen, L.W., C.W. Bostian, and G.E. Morgan. "Combining Electromagnetic Propagation, Geographic Information Systems, and Financial Modeling in a Software Package for Broadband Wireless Wide Area Network Design." Proceedings of the International Conference on Electromagnetics in Advanced Applications (ICEAA 01), pp.799-910, Torino, Italy, September 10-14, 2001.

Congalton, Russell, et al. "Update and Review of Accuracy Assessment Techniques for Remotely Sensed Data." Remote Sensing Research Report 83-1, January 1983.

Congalton, Russell, et al. "Analysis of Forest Classification Accuracy." Remote Sensing Research Report 81-1, February 1981.

Congalton, Russell G., and Green, Kass. *Assessing the Accuracy of Remotely Sensed Data: Principles and Practices.* New York: Lewis Publishers, 1999.

Corbley, Kevin P. "Wireless Communication Unes in with Satellite Imagery." Earth Observation Magazine. EOM Online Archives: August 1997.

Dodd, Howard Mannin. "The Validity of Using a Geographic Information System's Viewshed Function as a Predictor for the Reception of Line-of-Sight Radio Waves." MS thesis in Geography – Virginia Tech, 2001.

Gagne, Marissa. " An Analysis and Critique of DEM Creation and 3-D Modeling Using Airborne LiDAR and Photogrammetric Techniques." MS thesis in Civil Engineering – Virginia Tech, 2001.

Ohlson, Bjorn. "Remote Sensing Benefits Cellular Networks." Earth Observation Magazine. EOM Online Archives: November 1995.

Rose, Scott. "The Effect of Digital Elevation Model Resolution on Wave Propagation Predictions at 24 GHz." MS thesis in Geography – Virginia Tech, 2001.

Ruth, Mike. "Delivering Broadband: Geospatial Data for Wireless Network Design." Geospatial Solutions, September 2001 (p. 26-33).

Spencer, Ryan. "Modeling and Measuring GIS Viewshed Processing Speed on Different Digital Elevation Model Resolutions for Line of Sight Radio Wave Propagation." MS project in Geography – Virginia Tech, 2002.

Virginia Polytechnic Institute and State University. *LMDS at Virginia Tech* VT LMDS Group, 2001. http://www.lmds.vt.edu/

Weisman, Carl J. *The Essential Guide to RF and Wireless.* New Jersey: Prentice Hall PTR, 2000.

Appendix A – Final 16 Grids

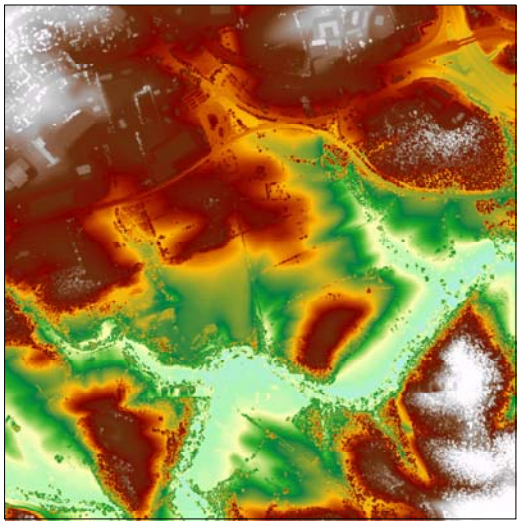

1m LiDAR Grid

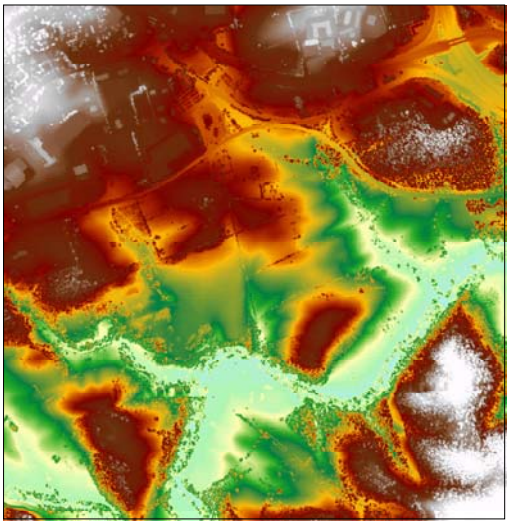

2m LiDAR Grid

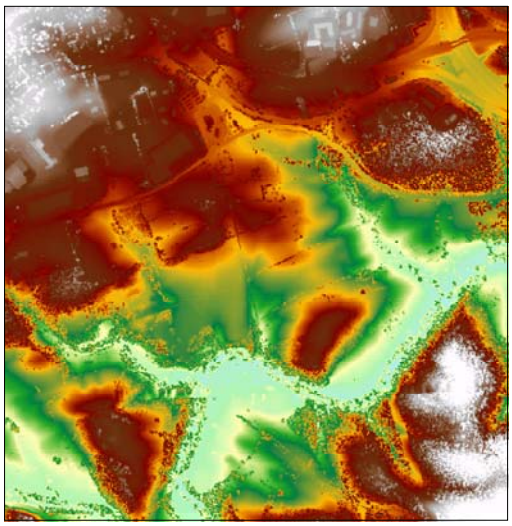

4m LiDAR Grid

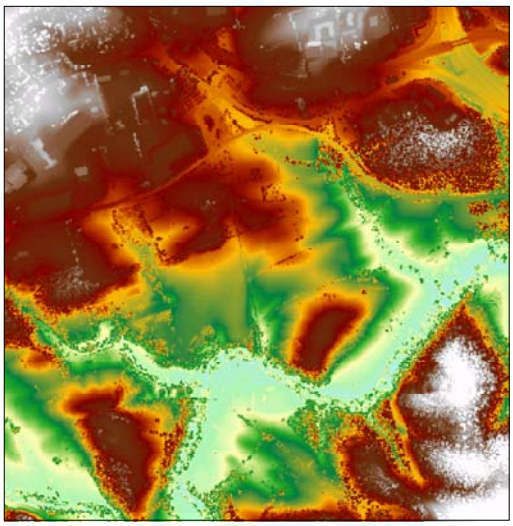

5m LiDAR Grid

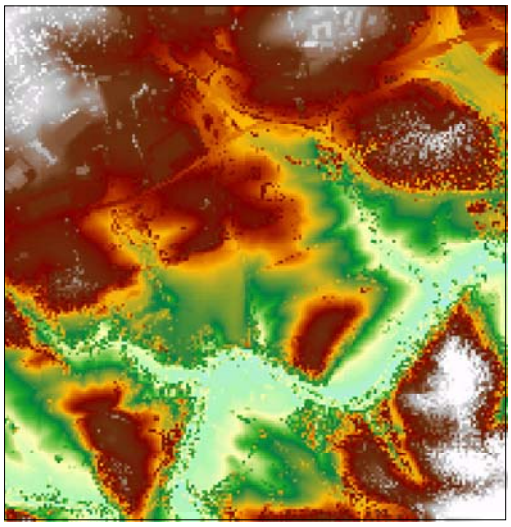

10m LiDAR Grid

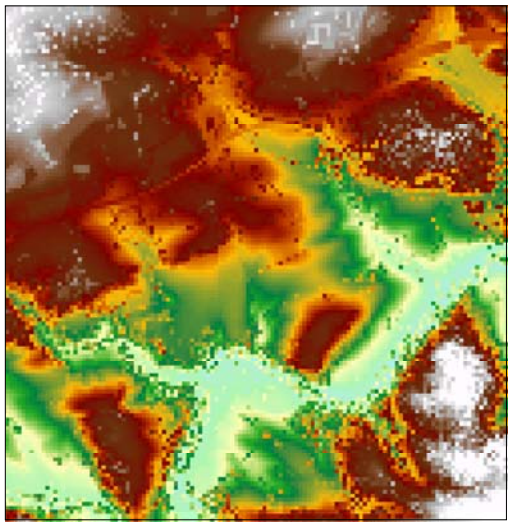

15m LiDAR Grid

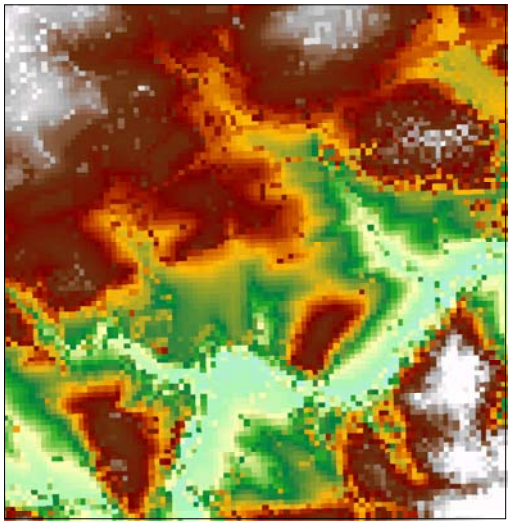

20m LiDAR Grid

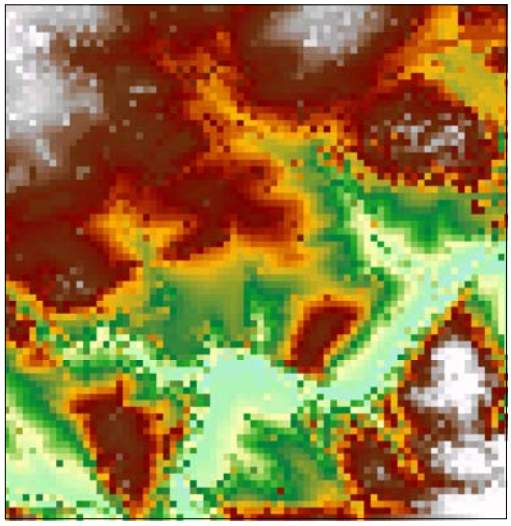

25m LiDAR Grid

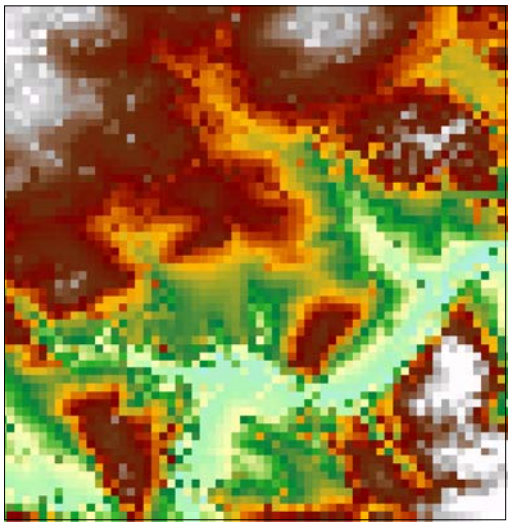

30m LiDAR Grid

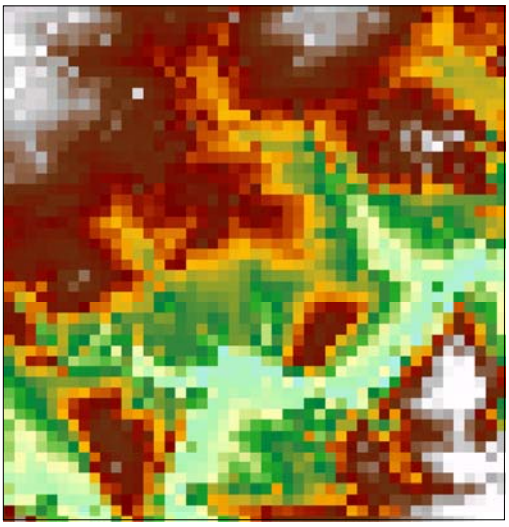

40m LiDAR Grid

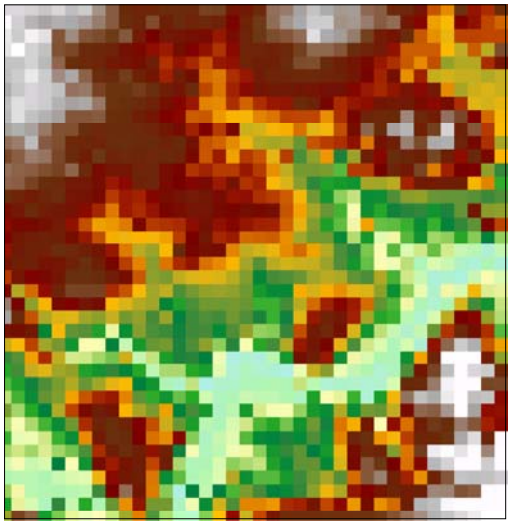

50m LiDAR Grid

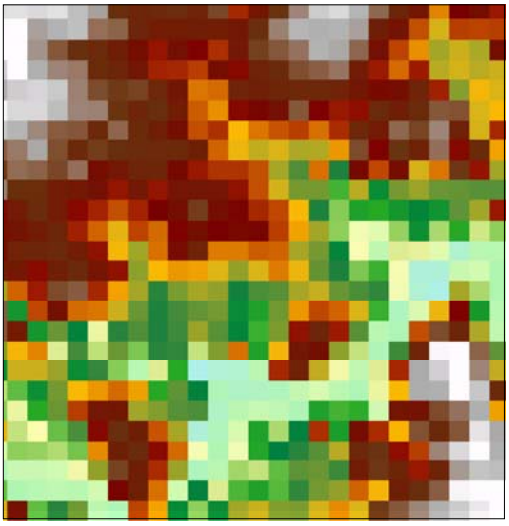

75m LiDAR Grid

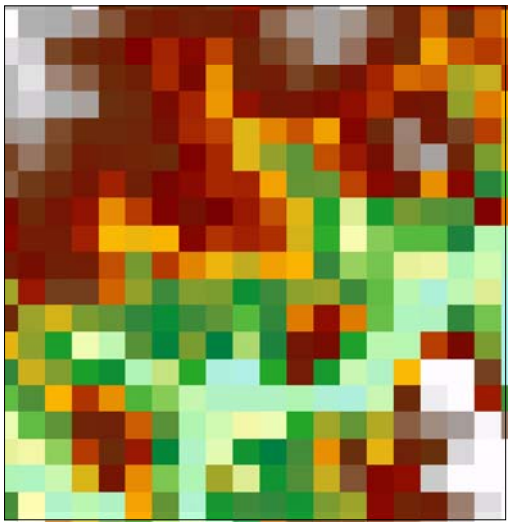

100m LiDAR Grid

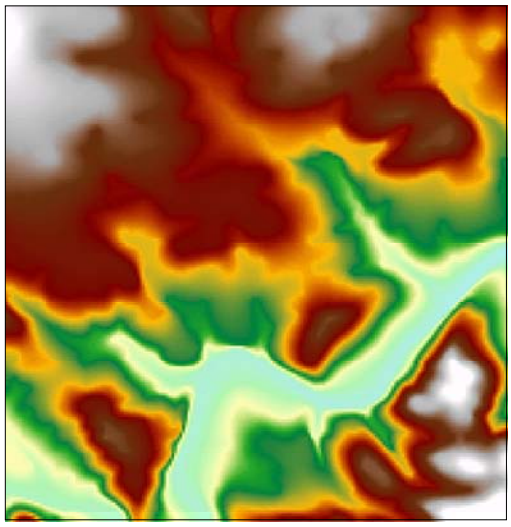

10m Bare-Earth Grid

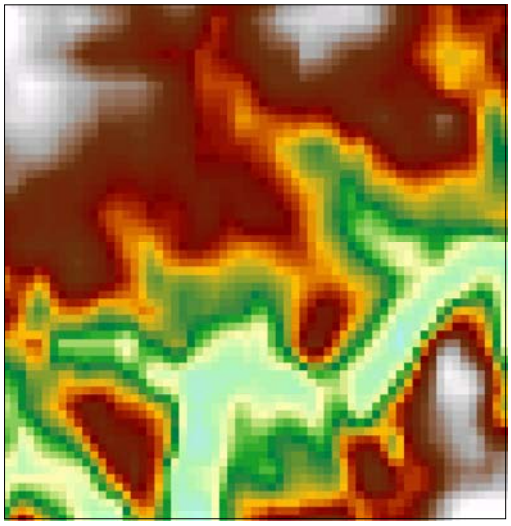

30m Bare-Earth Grid

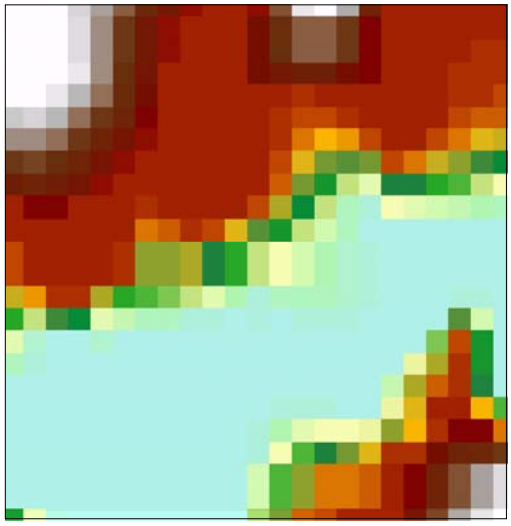

100m Bare-Earth Grid

Appendix B – Collected Field Data

Point ID	Signal Strength (dBm)	Antenna Visible?	Obstructions?
1	-10.10	yes	none
2	-9.20	yes	none
3	-10.40	yes	none
4	-15.20	yes	none
5	-15.50	yes	none
6	-18.20	yes	none
7	-16.90	yes	none
8	-16.90	yes	none
9	-18.90	yes	none
10	-19.90	yes	none
11	-20.10	yes	none
12	-18.10	yes	none
13	-20.10	yes	none
14	-29.10	partial	ground
15	-38.10	no	ground
16	-43.10	no	ground
17	-41.20	no	ground
18	-22.80	yes	none
19	-20.10	yes	none
20	-23.60	yes	none
21	-27.20	yes	none
22	-29.90	partial	ground/building
23	-36.60	no	building
24	-21.20	partial	ground/building
25	-45.40	no	building
26	-27.30	partial	ground/building
27	-47.20	no	ground/building
28	-50.10	no	ground
29	-49.30	no	building
30	-52.10	no	building
31	-46.10	no	building
32	-39.30	partial	vegetation
33	-34.20	partial	vegetation
34	-23.70	yes	none
35	-30.90	yes	none
36	-46.50	no	vegetation
37	-49.70	no	vegetation
38	-37.10	no	vegetation
39	-29.30	yes	none
40	-31.30	yes	none
41	-46.60	no	vegetation
42	-37.10	no	building
43	-34.60	no	vegetation
44	-38.50	no	vegetation
45	-28.70	yes	none

46	-32.10	partial	building
47	-46.70	no	building
48	-41.20	no	building
49	-41.60	no	ground
50	-45.90	no	vegetation
51	-50.30	no	vegetation
52	-58.80	no	vegetation
53	-65.10	no	vegetation
54	-46.80	no	vegetation
55	-56.60	no	building
56	-46.50	partial	vegetation
57	-27.90	partial	vegetation
58	-32.20	partial	vegetation
59	-33.30	partial	vegetation
60	-52.60	no	building
61	-25.70	partial	vegetation
62	-43.20	partial	vegetation
63	-58.30	no	building
64	-41.30	partial	vegetation
65	-21.40	partial	vegetation
66	-28.40	partial	vegetation
67	-24.60	partial	vegetation
68	-28.50	partial	vegetation
69	-24.30	partial	vegetation
70	-34.20	partial	vegetation
71	-53.80	no	building
72	-30.10	yes	none
73	-25.80	yes	none
74	-31.60	partial	vegetation
75	-45.60	no	vegetation
76	-53.20	no	vegetation
77	-45.60	no	vegetation
78	-56.50	no	building
79	-34.60	partial	vegetation
80	-51.20	no	building
81	-50.50	no	building
82	-47.60	no	vegetation
83	-39.20	yes	none
84	-33.20	yes	none
85	-36.20	yes	none
86	-53.80	no	building
87	-39.10	partial	building
88	-29.00	yes	none
89	-26.70	yes	none
90	-37.80	yes	none
91	-28.10	partial	vegetation
92	-41.90	no	vegetation
93	-25.70	yes	none
94	-25.70	yes	none
95	-25.10	yes	none
96	-33.20	yes	none
97	-30.20	yes	none

98	-42.40	no	building
99	-25.80	yes	none
100	-29.30	yes	none
101	-37.60	no	vegetation

Appendix C – Measured Signal Strength to LOS/NLOS

Point ID	Antenna Visible?	Obstructions?	Distance (feet)	Distance (meters)	Measured Signal Strength (dBm)	Predicted Signal Strength (dBm)	Difference	LOS? (<3dB)	LOS? (<6dB)	LOS? (<9dB)	LOS? (<12dB)
1	yes	none	125.43	38.2	-10.1	-6.9	3.2	no	yes	yes	yes
2	**yes**	**none**	**162.58**	**49.6**	**-9.2**	**-9.2**	**0.0**	yes	yes	yes	yes
3	yes	none	159.01	48.5	-10.4	-9.0	1.4	yes	yes	yes	yes
4	yes	none	173.34	52.8	-15.2	-9.7	5.5	no	yes	yes	yes
5	yes	none	196.62	59.9	-15.5	-10.8	4.7	no	yes	yes	yes
6	yes	none	228.54	69.7	-18.2	-12.1	6.1	no	no	yes	yes
7	yes	none	253.14	77.2	-16.9	-13.0	3.9	no	yes	yes	yes
8	yes	none	273.80	83.5	-16.9	-13.7	3.2	no	yes	yes	yes
9	yes	none	287.91	87.8	-18.9	-14.2	4.7	no	yes	yes	yes
10	yes	none	307.06	93.6	-19.9	-14.7	5.2	no	yes	yes	yes
11	yes	none	305.34	93.1	-20.1	-14.7	5.4	no	yes	yes	yes
12	yes	none	306.78	93.5	-18.1	-14.7	3.4	no	yes	yes	yes
13	yes	none	303.70	92.6	-20.1	-14.6	5.5	no	yes	yes	yes
14	partial	ground	257.72	78.6	-29.1	-13.2	15.9	no	no	no	no
15	no	ground	268.66	81.9	-38.1	-13.6	24.5	no	no	no	no
16	no	ground	279.54	85.2	-43.1	-13.9	29.2	no	no	no	no
17	no	ground	298.30	90.9	-41.2	-14.5	26.7	no	no	no	no
18	yes	none	350.94	107.0	-22.8	-15.9	6.9	no	no	yes	yes
19	yes	none	381.94	116.4	-20.1	-16.6	3.5	no	yes	yes	yes
20	yes	none	394.67	120.3	-23.6	-16.9	6.7	no	no	yes	yes
21	yes	none	393.43	119.9	-27.2	-16.9	10.3	no	no	no	yes
22	partial	ground/bldg	395.64	120.6	-29.9	-16.9	13.0	no	no	no	no
23	no	building	461.66	140.7	-36.6	-18.3	18.3	no	no	no	no
24	partial	ground/bldg	492.44	150.1	-21.2	-18.8	2.4	yes	yes	yes	yes
25	no	building	517.73	157.8	-45.4	-19.3	26.1	no	no	no	no
26	partial	ground/bldg	565.13	172.3	-27.3	-20.0	7.3	no	no	yes	yes
27	no	ground/bldg	630.81	192.3	-47.2	-21.0	26.2	no	no	no	no
28	no	ground	602.83	183.7	-50.1	-20.6	29.5	no	no	no	no
29	no	building	553.60	168.7	-49.3	-19.8	29.5	no	no	no	no
30	no	building	481.61	146.8	-52.1	-18.6	33.5	no	no	no	no
31	no	building	444.30	135.4	-46.1	-17.9	28.2	no	no	no	no
32	partial	vegetation	494.02	150.6	-39.3	-18.8	20.5	no	no	no	no
33	partial	vegetation	552.24	168.3	-34.2	-19.8	14.4	no	no	no	no
34	yes	none	630.40	192.1	-23.7	-21.0	2.7	yes	yes	yes	yes
35	yes	none	724.51	220.8	-30.9	-22.2	8.7	no	no	yes	yes
36	no	vegetation	770.23	234.8	-46.5	-22.7	23.8	no	no	no	no
37	no	vegetation	775.20	236.3	-49.7	-22.8	26.9	no	no	no	no
38	no	vegetation	791.29	241.2	-37.1	-22.9	14.2	no	no	no	no
39	yes	none	414.56	126.4	-29.3	-17.3	12.0	no	no	no	yes
40	yes	none	398.51	121.5	-31.3	-17.0	14.3	no	no	no	no
41	no	vegetation	403.61	123.0	-46.6	-17.1	29.5	no	no	no	no
42	no	building	427.28	130.2	-37.1	-17.6	19.5	no	no	no	no
43	no	vegetation	448.52	136.7	-34.6	-18.0	16.6	no	no	no	no
44	no	vegetation	449.39	137.0	-38.5	-18.0	20.5	no	no	no	no
45	yes	none	438.40	133.6	-28.7	-17.8	10.9	no	no	no	yes
46	partial	building	417.88	127.4	-32.1	-17.4	14.7	no	no	no	no
47	no	building	426.33	129.9	-46.7	-17.6	29.1	no	no	no	no
48	no	building	444.21	135.4	-41.2	-17.9	23.3	no	no	no	no
49	no	ground	448.25	136.6	-41.6	-18.0	23.6	no	no	no	no
50	no	vegetation	491.86	149.9	-45.9	-18.8	27.1	no	no	no	no
51	no	vegetation	545.54	166.3	-50.3	-19.7	30.6	no	no	no	no
52	no	vegetation	656.47	200.1	-58.8	-21.3	37.5	no	no	no	no
53	no	vegetation	892.45	272.0	-65.1	-24.0	41.1	no	no	no	no
54	no	vegetation	1015.50	309.5	-46.8	-25.1	21.7	no	no	no	no
55	no	building	849.31	258.9	-56.6	-23.6	33.0	no	no	no	no
56	partial	vegetation	579.32	176.6	-46.5	-20.2	26.3	no	no	no	no
57	partial	vegetation	714.65	217.8	-27.9	-22.1	5.8	no	yes	yes	yes
58	partial	vegetation	774.29	236.0	-32.2	-22.7	9.5	no	no	no	yes
59	partial	vegetation	706.47	215.3	-33.3	-22.0	11.3	no	no	no	yes
60	no	building	690.98	210.6	-52.6	-21.8	30.8	no	no	no	no
61	partial	vegetation	698.03	212.8	-25.7	-21.8	3.9	no	yes	yes	yes
62	partial	vegetation	593.35	180.9	-43.2	-20.4	22.8	no	no	no	no
63	no	building	556.76	169.7	-58.3	-19.9	38.4	no	no	no	no
64	partial	vegetation	593.31	180.8	-41.3	-20.4	20.9	no	no	no	no
65	partial	vegetation	585.89	178.6	-21.4	-20.3	1.1	yes	yes	yes	yes

66	partial	vegetation	507.08	154.6	-28.4	-19.1	9.3	no	no	no	yes
67	partial	vegetation	473.95	144.5	-24.6	-18.5	6.1	no	no	yes	yes
68	partial	vegetation	548.51	167.2	-28.5	-19.8	8.7	no	no	yes	yes
69	partial	vegetation	684.55	208.7	-24.3	-21.7	2.6	yes	yes	yes	yes
70	partial	vegetation	722.27	220.1	-34.2	-22.1	12.1	no	no	no	no
71	no	building	760.59	231.8	-53.8	-22.6	31.2	no	no	no	no
72	yes	none	1048.25	319.5	-30.1	-25.4	4.7	no	yes	yes	yes
73	yes	none	948.71	289.2	-25.8	-24.5	1.3	yes	yes	yes	yes
74	partial	vegetation	921.77	281.0	-31.6	-24.3	7.3	no	no	yes	yes
75	no	vegetation	903.89	275.5	-45.6	-24.1	21.5	no	no	no	no
76	no	vegetation	955.05	291.1	-53.2	-24.6	28.6	no	no	no	no
77	no	vegetation	1045.73	318.7	-45.6	-25.4	20.2	no	no	no	no
78	no	building	1052.94	320.9	-56.5	-25.4	31.1	no	no	no	no
79	partial	vegetation	1064.49	324.5	-34.6	-25.5	9.1	no	no	no	yes
80	no	building	1138.93	347.1	-51.2	-26.1	25.1	no	no	no	no
81	no	building	1253.81	382.2	-50.5	-26.9	23.6	no	no	no	no
82	no	vegetation	1177.13	358.8	-47.6	-26.4	21.2	no	no	no	no
83	yes	none	1100.98	335.6	-39.2	-25.8	13.4	no	no	no	no
84	yes	none	1092.44	333.0	-33.2	-25.7	7.5	no	no	yes	yes
85	yes	none	1190.99	363.0	-36.2	-26.5	9.7	no	no	no	yes
86	no	building	1325.97	404.2	-53.8	-27.4	26.4	no	no	no	no
87	partial	building	1340.64	408.6	-39.1	-27.5	11.6	no	no	no	yes
88	yes	none	1266.26	386.0	-29.0	-27.0	2.0	yes	yes	yes	yes
89	yes	none	1050.31	320.1	-26.7	-25.4	1.3	yes	yes	yes	yes
90	yes	none	1038.39	316.5	-37.8	-25.3	12.5	no	no	no	no
91	partial	vegetation	1037.28	316.2	-28.1	-25.3	2.8	yes	yes	yes	yes
92	no	vegetation	953.50	290.6	-41.9	-24.6	17.3	no	no	no	no
93	yes	none	937.12	285.6	-25.7	-24.4	1.3	yes	yes	yes	yes
94	yes	none	929.38	283.3	-25.7	-24.3	1.4	yes	yes	yes	yes
95	yes	none	947.96	288.9	-25.1	-24.5	0.6	yes	yes	yes	yes
96	yes	none	936.88	285.6	-33.2	-24.4	8.8	no	no	yes	yes
97	yes	none	957.85	292.0	-30.2	-24.6	5.6	no	yes	yes	yes
98	no	building	885.20	269.8	-42.4	-23.9	18.5	no	no	no	no
99	yes	none	853.11	260.0	-25.8	-23.6	2.2	yes	yes	yes	yes
100	yes	none	836.70	255.0	-29.3	-23.4	5.9	no	yes	yes	yes
101	no	vegetation	835.20	254.6	-37.6	-23.4	14.2	no	no	no	no

Appendix D – Predicted Commsheds

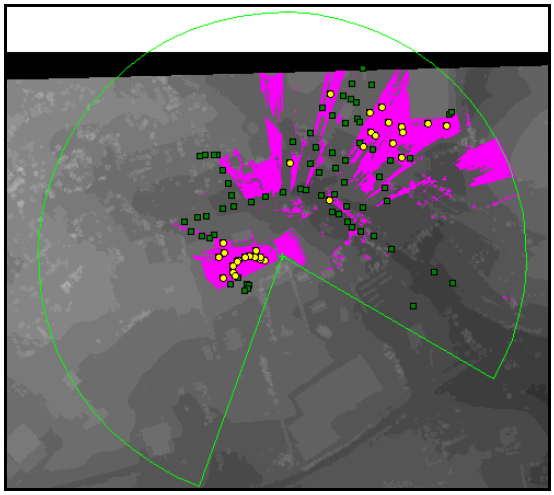

1m LiDAR Predicted Commshed

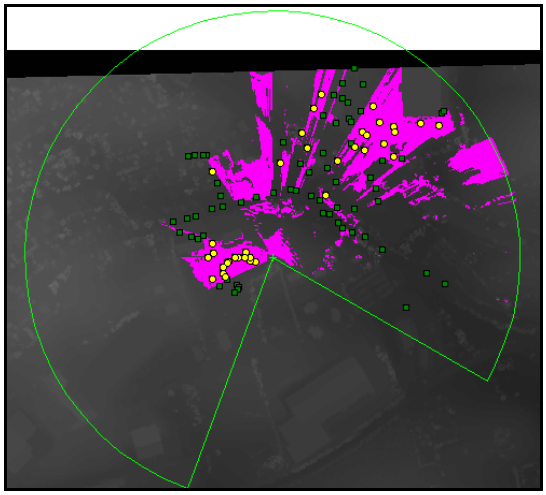

2m LiDAR Predicted Commshed

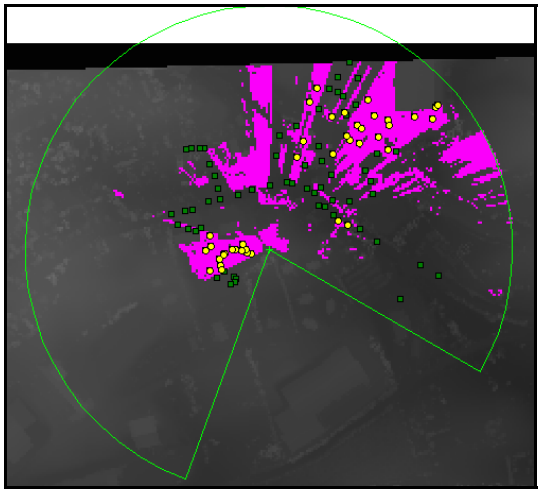

4m LiDAR Predicted Commshed

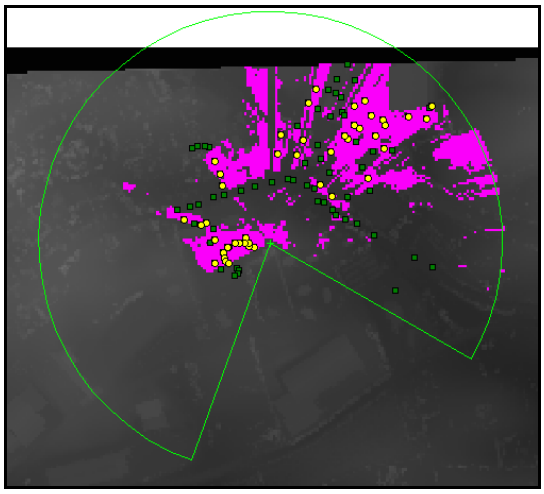

5m LiDAR Predicted Commshed

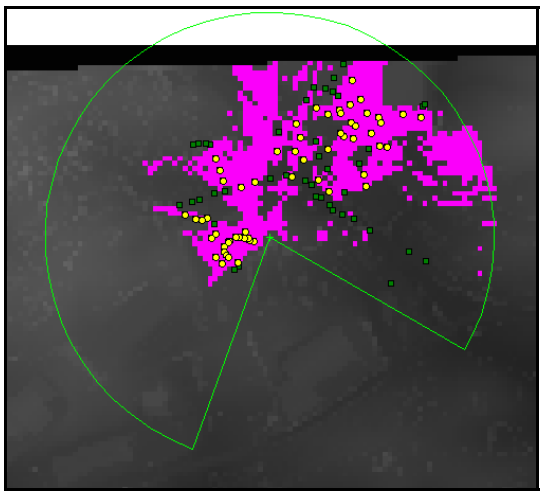

10m LiDAR Predicted Commshed

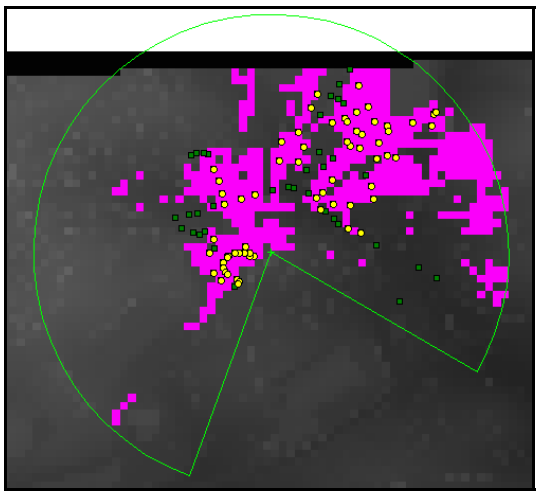

15m LiDAR Predicted Commshed

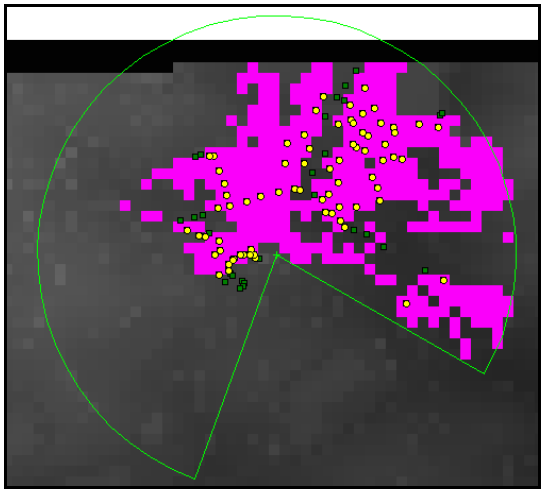

20m LiDAR Predicted Commshed

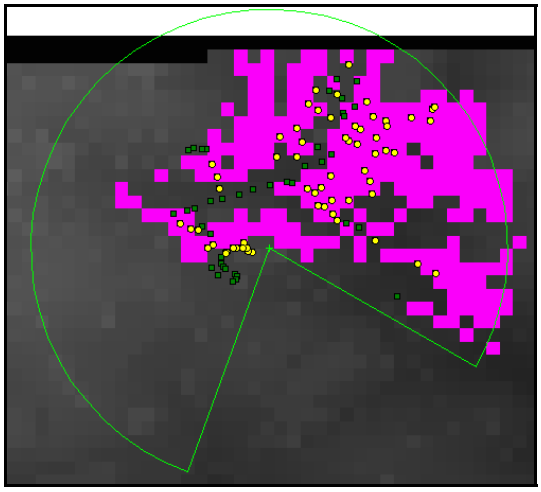

25m LiDAR Predicted Commshed

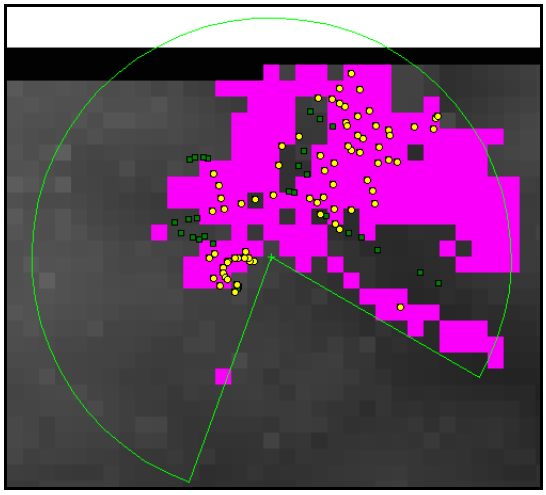

30m LiDAR Predicted Commshed

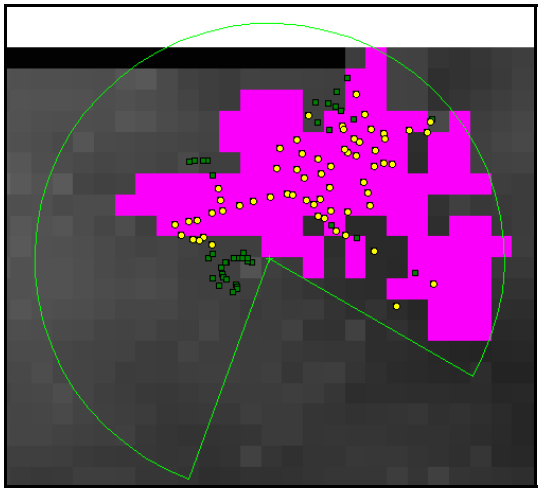

40m LiDAR Predicted Commshed

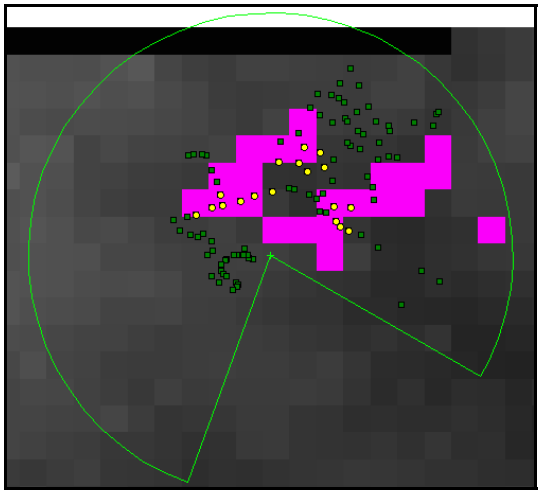

50m LiDAR Predicted Commshed

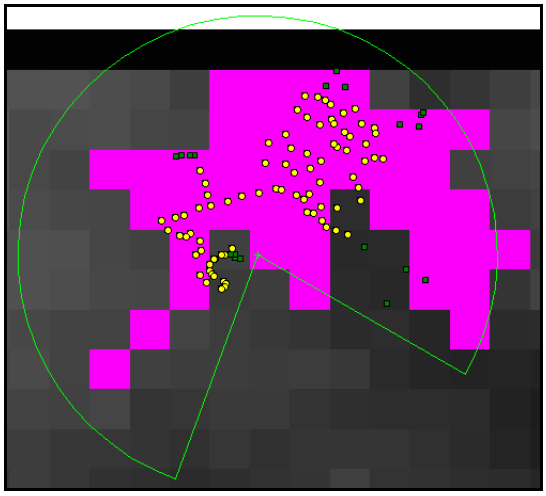

75m LiDAR Predicted Commshed

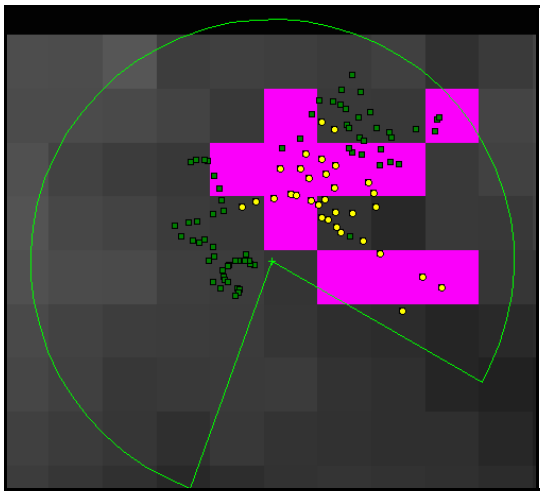

100m LiDAR Predicted Commshed

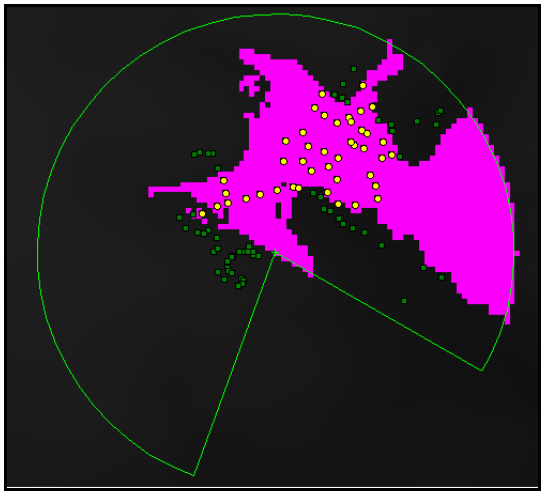

10m Bare-Earth Commshed

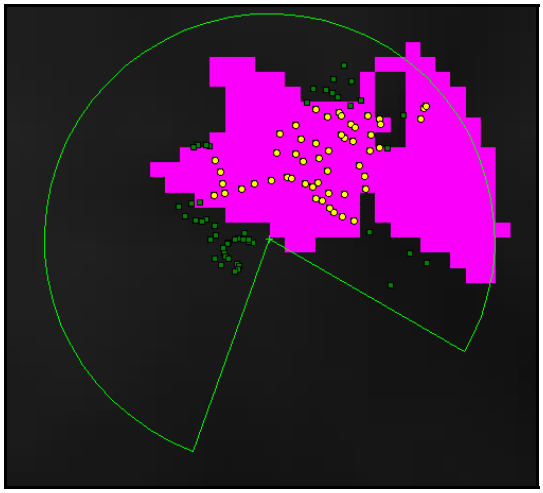

30m Bare-Earth Commshed

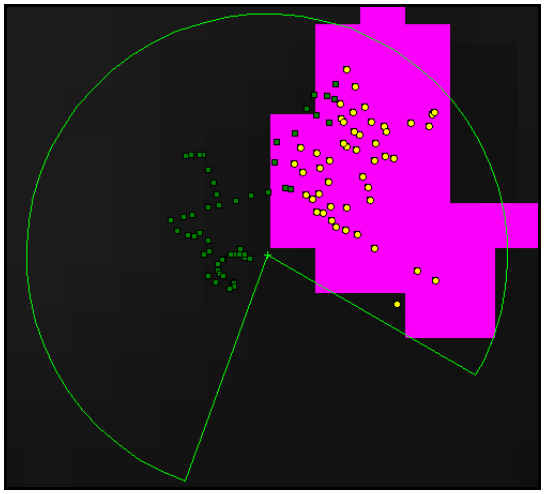

100m Bare-Earth Commshed

Appendix E – Overall Accuracy and Khat Scores for each Grid

	1m	2m	4m	5m	10m	15m	20m	25m	30m	40m	50m	75m	100m	10mBE	30mBE	100mBE
Viewshed Predicted In	31	34	40	45	58	65	73	61	73	62	18	82	32	43	52	48
Viewshed Predicted Out	70	67	61	56	43	36	28	40	28	39	83	19	69	58	49	53
Correctly Predicted In	8	10	9	11	12	13	14	13	12	10	0	11	2	8	9	9
Correctly Predicted Out	64	63	56	53	41	35	28	39	26	35	69	16	57	52	44	48
Incorrectly Predicted In	23	24	31	34	46	52	59	48	61	52	18	71	30	35	43	39
Incorrectly Predicted Out	6	4	5	3	2	1	0	1	2	4	14	3	12	6	5	5
Total Correctly Predicted	72	73	65	64	53	48	42	52	38	45	69	27	59	60	53	57
Total Incorrectly Predicted	29	28	36	37	48	53	59	49	63	56	32	74	42	41	48	44
Total Points (101pts)	101	101	101	101	101	101	101	101	101	101	101	101	101	101	101	101
Overall Accuracy	71.29%	72.28%	64.36%	63.37%	52.48%	47.52%	41.58%	51.49%	37.62%	44.55%	68.32%	26.73%	58.42%	59.41%	52.48%	56.44%
Khat (%)	20.34%	27.41%	16.11%	20.47%	14.16%	13.09%	11.63%	15.65%	5.64%	4.78%	-18.48%	-1.00%	-13.12%	9.05%	6.95%	9.64%
Khat	0.20	0.27	0.16	0.20	0.14	0.13	0.12	0.16	0.06	0.05	-0.18	-0.01	-0.13	0.09	0.07	0.10
Z Score	1.65	2.28	1.23	1.58	0.97	0.86	0.73	1.08	0.33	0.29	-3.82	-0.05	-1.00	0.64	0.46	0.67

-3dB Threshold

	1m	2m	4m	5m	10m	15m	20m	25m	30m	40m	50m	75m	100m	10mBE	30mBE	100mBE
Viewshed Predicted In	31	34	40	45	58	65	73	61	73	62	18	82	32	43	52	48
Viewshed Predicted Out	70	67	61	56	43	36	28	40	28	39	83	19	69	58	49	53
Correctly Predicted In	20	23	22	26	26	28	27	23	28	14	0	25	3	12	12	12
Correctly Predicted Out	60	60	53	52	39	34	25	33	26	23	53	14	42	40	31	35
Incorrectly Predicted In	11	11	18	19	32	37	46	38	45	48	18	57	29	31	40	36
Incorrectly Predicted Out	10	7	8	4	4	2	3	7	2	16	30	5	27	18	18	18
Total Correctly Predicted	80	83	75	78	65	62	52	56	54	37	53	39	45	52	43	47
Total Incorrectly Predicted	21	18	26	23	36	39	49	45	47	64	48	62	56	49	58	54
Total Points (101pts)	101	101	101	101	101	101	101	101	101	101	101	101	101	101	101	101
Overall Accuracy	79.21%	82.18%	74.26%	77.23%	64.36%	61.39%	51.49%	55.45%	53.47%	36.63%	52.48%	38.61%	44.55%	51.49%	42.57%	46.53%
Khat (%)	50.69%	58.91%	43.77%	52.35%	32.77%	30.83%	17.83%	17.83%	21.19%	-16.01%	-28.66%	2.03%	-30.26%	-3.25%	-13.48%	-9.12%
Khat	0.51	0.59	0.44	0.52	0.33	0.31	0.18	0.18	0.21	-0.16	-0.29	0.02	-0.30	-0.03	-0.13	-0.09
Z Score	5.42	6.80	4.63	5.97	3.14	2.81	1.34	1.47	1.65	-1.01	-3.02	0.12	-3.91	-0.29	-1.02	-0.75

-6dB Threshold

	1m	2m	4m	5m	10m	15m	20m	25m	30m	40m	50m	75m	100m	10mBE	30mBE	100mBE
Viewshed Predicted In	31	34	40	45	58	65	73	61	73	62	18	82	32	43	52	48
Viewshed Predicted Out	70	67	61	56	43	36	28	40	28	39	83	19	69	58	49	53
Correctly Predicted In	24	27	26	31	34	35	35	31	35	19	2	34	6	16	17	16
Correctly Predicted Out	54	54	47	47	37	31	23	31	23	18	45	13	35	34	26	29
Incorrectly Predicted In	7	7	14	14	24	30	38	30	38	43	16	48	26	27	35	32
Incorrectly Predicted Out	16	13	14	9	6	5	5	9	5	21	38	6	34	24	23	24
Total Correctly Predicted	78	81	73	78	71	66	58	62	58	37	47	47	41	50	43	45
Total Incorrectly Predicted	23	20	28	23	30	35	43	39	43	64	54	54	60	51	58	56
Total Points (101pts)	101	101	101	101	101	101	101	101	101	101	101	101	101	101	101	101
Overall Accuracy	77.23%	80.20%	72.28%	77.23%	70.30%	65.35%	57.43%	61.39%	57.43%	36.63%	46.53%	46.53%	40.59%	49.50%	42.57%	44.55%
Khat (%)	50.48%	57.51%	42.05%	53.40%	42.37%	34.60%	22.07%	25.97%	22.07%	-21.00%	-23.45%	5.35%	-28.61%	-4.21%	-14.15%	-12.04%
Khat	0.50	0.58	0.42	0.53	0.42	0.35	0.22	0.26	0.22	-0.21	-0.23	0.05	-0.29	-0.04	-0.14	-0.12
Z Score	5.60	6.81	4.56	6.27	4.60	3.44	1.86	2.48	1.86	-1.55	-1.65	0.35	-2.95	-0.42	-1.29	-1.16

-9dB Threshold

	1m	2m	4m	5m	10m	15m	20m	25m	30m	40m	50m	75m	100m	10mBE	30mBE	100mBE
Viewshed Predicted In	31	34	40	45	58	65	73	61	73	62	18	82	32	43	52	48
Viewshed Predicted Out	70	67	61	56	43	36	28	40	28	39	83	19	69	58	49	53
Correctly Predicted In	27	30	30	36	40	42	42	38	43	25	4	41	10	20	23	21
Correctly Predicted Out	48	48	42	43	34	29	21	29	22	15	38	11	30	29	23	25
Incorrectly Predicted In	4	4	10	9	18	23	31	23	30	37	14	41	22	23	29	27
Incorrectly Predicted Out	22	19	19	13	9	7	7	11	6	24	45	8	39	29	26	28
Total Correctly Predicted	75	78	72	79	74	71	63	67	65	40	42	52	40	49	46	46
Total Incorrectly Predicted	26	23	29	22	27	30	38	34	36	61	59	49	61	52	55	55
Total Points (101pts)	101	101	101	101	101	101	101	101	101	101	101	101	101	101	101	101
Overall Accuracy	74.26%	77.23%	71.29%	78.22%	73.27%	70.30%	62.38%	66.34%	64.36%	39.60%	41.58%	51.49%	39.60%	48.51%	45.54%	45.54%
Khat (%)	47.92%	54.01%	42.22%	56.29%	46.77%	41.10%	25.74%	33.09%	29.64%	-19.98%	-19.11%	4.74%	-22.12%	-3.43%	-8.81%	-9.07%
Khat	0.48	0.54	0.42	0.56	0.47	0.41	0.26	0.33	0.30	-0.20	-0.19	0.05	-0.22	-0.03	-0.09	-0.09
Z Score	5.32	6.36	4.62	6.83	5.29	4.40	2.36	3.44	2.79	-1.77	-1.15	0.33	-1.80	-0.34	-0.88	-0.92

-12dB Threshold

	1m	2m	4m	5m	10m	15m	20m	25m	30m	40m	50m	75m	100m	10mBE	30mBE	100mBE
Viewshed Predicted In	28	30	35	31	42	47	53	43	55	43	11	59	19	26	34	35
Viewshed Predicted Out	49	47	42	46	35	30	24	34	22	34	66	18	58	51	43	42
Correctly Predicted In	28	30	29	29	33	35	33	28	35	17	2	30	3	11	14	14
Correctly Predicted Out	40	40	34	38	31	28	20	25	20	14	31	11	24	25	20	19
Incorrectly Predicted In	0	0	6	2	9	12	20	15	20	26	9	29	16	15	20	21
Incorrectly Predicted Out	9	7	8	8	4	2	4	9	2	20	35	7	34	26	23	23
Total Correctly Predicted	68	70	63	67	64	63	53	53	55	31	33	41	27	36	34	33
Total Incorrectly Predicted	9	7	14	10	13	14	24	24	22	46	44	36	50	41	43	44
Total Points (77pts)	77	77	77	77	77	77	77	77	77	77	77	77	77	77	77	77
Overall Accuracy	88.31%	90.91%	81.82%	87.01%	83.12%	81.82%	68.83%	68.83%	71.43%	40.26%	42.86%	53.25%	35.06%	46.75%	44.16%	42.86%
Khat (%)	76.37%	81.66%	63.51%	73.83%	66.35%	63.95%	38.56%	37.94%	43.80%	-18.94%	-17.56%	8.39%	-32.48%	-7.86%	-12.20%	-14.69%
Khat	0.76	0.82	0.64	0.74	0.66	0.64	0.39	0.38	0.44	-0.19	-0.18	0.08	-0.32	-0.08	-0.12	-0.15
Z Score	10.46	12.48	7.20	9.61	7.81	7.36	3.47	3.57	4.07	-1.60	-0.87	0.56	-1.90	-0.61	-1.07	-1.30

Visibility Threshold

Appendix F – Z Scores and Significance above chance for each grid

	Khat	Variance	Ind. Z Score	95%	Significant?
1m	0.2034	0.0151	1.6537	1.96	NOT SIG
2m	0.2741	0.0144	2.2838	1.96	**SIG**
4m	0.1611	0.0172	1.2278	1.96	NOT SIG
5m	0.2047	0.0169	1.5753	1.96	NOT SIG
10m	0.1416	0.0213	0.9699	1.96	NOT SIG
15m	0.1309	0.0231	0.8605	1.96	NOT SIG
20m	0.1163	0.0254	0.7301	1.96	NOT SIG
25m	0.1565	0.0212	1.0758	1.96	NOT SIG
30m	0.0564	0.0292	0.3298	1.96	NOT SIG
40m	0.0478	0.0270	0.2911	1.96	NOT SIG
50m	-0.1848	0.0023	-3.8216	1.96	NOT SIG
75m	-0.0100	0.0363	-0.0525	2.06	NOT SIG
100m	-0.1312	0.0171	-1.0033	2.09	NOT SIG
10mBE	0.0905	0.0197	0.6449	1.96	NOT SIG
30mBE	0.0695	0.0231	0.4575	1.96	NOT SIG
100mBE	0.0964	0.0209	0.6664	2.08	NOT SIG

-3dB Threshold

	Khat	Variance	Ind. Z Score	95%	Significant?
1m	0.5069	0.0087	5.4240	1.96	**SIG**
2m	0.5891	0.0075	6.8012	1.96	**SIG**
4m	0.4377	0.0089	4.6349	1.96	**SIG**
5m	0.5235	0.0077	5.9659	1.96	**SIG**
10m	0.3277	0.0109	3.1382	1.96	**SIG**
15m	0.3083	0.0121	2.8075	1.96	**SIG**
20m	0.1783	0.0177	1.3404	1.96	NOT SIG
25m	0.1783	0.0147	1.4717	1.96	NOT SIG
30m	0.2119	0.0164	1.6530	1.96	NOT SIG
40m	-0.1601	0.0250	-1.0124	1.96	NOT SIG
50m	-0.2866	0.0090	-3.0170	1.96	NOT SIG
75m	0.0203	0.0287	0.1200	2.06	NOT SIG
100m	-0.3026	0.0060	-3.9133	2.09	NOT SIG
10mBE	-0.0325	0.0122	-0.2943	1.96	NOT SIG
30mBE	-0.1348	0.0174	-1.0208	1.96	NOT SIG
100mBE	-0.0912	0.0147	-0.7532	2.08	NOT SIG

-6dB Threshold

	Khat	Variance	Ind. Z Score	95%	Significant?
1m	0.5048	0.0081	5.6048	1.96	**SIG**
2m	0.5751	0.0071	6.8072	1.96	**SIG**
4m	0.4205	0.0085	4.5623	1.96	**SIG**
5m	0.5340	0.0073	6.2669	1.96	**SIG**
10m	0.4237	0.0085	4.5971	1.96	**SIG**
15m	0.3460	0.0101	3.4437	1.96	**SIG**
20m	0.2207	0.0141	1.8561	1.96	NOT SIG
25m	0.2597	0.0109	2.4832	1.96	**SIG**
30m	0.2207	0.0141	1.8561	1.96	NOT SIG
40m	-0.2100	0.0184	-1.5500	1.96	NOT SIG
50m	-0.2345	0.0203	-1.6467	1.96	NOT SIG
75m	0.0535	0.0235	0.3485	2.06	NOT SIG
100m	-0.2861	0.0094	-2.9544	2.09	NOT SIG
10mBE	-0.0421	0.0100	-0.4218	1.96	NOT SIG
30mBE	-0.1415	0.0121	-1.2870	1.96	NOT SIG
100mBE	-0.1204	0.0107	-1.1632	2.08	NOT SIG

-9dB Threshold

	Khat	Variance	Ind. Z Score	95%	Significant?
1m	0.4792	0.0081	5.3177	1.96	**SIG**
2m	0.5401	0.0072	6.3624	1.96	**SIG**
4m	0.4222	0.0083	4.6208	1.96	**SIG**
5m	0.5629	0.0068	6.8311	1.96	**SIG**
10m	0.4677	0.0078	5.2916	1.96	**SIG**
15m	0.4110	0.0087	4.4039	1.96	**SIG**
20m	0.2574	0.0119	2.3561	1.96	**SIG**
25m	0.3309	0.0093	3.4366	1.96	**SIG**
30m	0.2964	0.0113	2.7930	1.96	**SIG**
40m	-0.1998	0.0127	-1.7743	1.96	NOT SIG
50m	-0.1911	0.0276	-1.1499	1.96	NOT SIG
75m	0.0474	0.0206	0.3301	2.06	NOT SIG
100m	-0.2212	0.0150	-1.8040	2.09	NOT SIG
10mBE	-0.0343	0.0103	-0.3369	1.96	NOT SIG
30mBE	-0.0881	0.0100	-0.8833	1.96	NOT SIG
100mBE	-0.0907	0.0098	-0.9150	2.08	NOT SIG

-12dB Threshold

	Khat	Variance	Ind. Z Score	95%	Significant?
1m	0.7637	0.0053	10.4570	1.96	**SIG**
2m	0.8166	0.0043	12.4823	1.96	**SIG**
4m	0.6351	0.0078	7.2018	1.96	**SIG**
5m	0.7383	0.0059	9.6124	1.96	**SIG**
10m	0.6635	0.0072	7.8097	1.96	**SIG**
15m	0.6395	0.0075	7.3615	1.96	**SIG**
20m	0.3856	0.0123	3.4706	1.96	**SIG**
25m	0.3794	0.0113	3.5718	1.96	**SIG**
30m	0.4380	0.0116	4.0694	1.96	**SIG**
40m	-0.1894	0.0140	-1.5980	1.96	NOT SIG
50m	-0.1756	0.0408	-0.8690	1.96	NOT SIG
75m	0.0839	0.0224	0.5604	2.06	NOT SIG
100m	-0.3248	0.0292	-1.9013	2.09	NOT SIG
10mBE	-0.0786	0.0168	-0.6057	1.96	NOT SIG
30mBE	-0.1220	0.0131	-1.0666	1.96	NOT SIG
100mBE	-0.1469	0.0128	-1.2974	2.08	NOT SIG

Visibility Threshold

Appendix G – Significance among Grids

	1m	2m	4m	5m	10m	15m	20m	25m	30m	40m	50m	75m	100m	10mBE	30mBE	100mBE
1m	NOT															
2m	NOT	NOT														
4m	NOT	NOT	NOT													
5m	NOT	NOT	NOT	NOT												
10m	NOT	NOT	NOT	NOT	NOT											
15m	NOT	NOT	NOT	NOT	NOT	NOT										
20m	NOT	NOT	NOT	NOT	NOT	NOT	NOT									
25m	NOT	NOT	NOT	NOT	NOT	NOT	NOT	NOT								
30m	NOT	NOT	NOT	NOT	NOT	NOT	NOT	NOT	NOT							
40m	NOT	NOT	NOT	NOT	NOT	NOT	NOT	NOT	NOT	NOT						
50m	SIG	SIG	SIG	SIG	SIG	SIG	NOT	SIG	NOT	NOT	NOT					
75m	NOT	NOT	NOT	NOT	NOT	NOT	NOT	NOT	NOT	NOT	NOT	NOT				
100m	NOT	SIG	NOT	NOT	NOT	NOT	NOT	NOT	NOT	NOT	NOT	NOT	NOT			
10mBE	NOT	NOT	NOT	NOT	NOT	NOT	NOT	NOT	NOT	NOT	NOT	NOT	NOT	NOT		
30mBE	NOT	NOT	NOT	NOT	NOT	NOT	NOT	NOT	NOT	NOT	NOT	NOT	NOT	NOT	NOT	
100mBE	NOT	NOT	NOT	NOT	NOT	NOT	NOT	NOT	NOT	NOT	NOT	NOT	NOT	NOT	NOT	NOT

-3dB Threshold

	1m	2m	4m	5m	10m	15m	20m	25m	30m	40m	50m	75m	100m	10mBE	30mBE	100mBE
1m	NOT															
2m	NOT	NOT														
4m	NOT	NOT	NOT													
5m	NOT	NOT	NOT	NOT												
10m	NOT	NOT	NOT	NOT	NOT											
15m	NOT	SIG	NOT	NOT	NOT	NOT										
20m	SIG	SIG	NOT	SIG	NOT	NOT	NOT									
25m	SIG	SIG	NOT	SIG	NOT	NOT	NOT	NOT								
30m	NOT	SIG	NOT	SIG	NOT	NOT	NOT	NOT	NOT							
40m	SIG	SIG	SIG	SIG	SIG	SIG	NOT	NOT	NOT	NOT						
50m	SIG	SIG	SIG	SIG	SIG	SIG	SIG	SIG	SIG	NOT	NOT					
75m	SIG	SIG	SIG	SIG	NOT	NOT	NOT	NOT	NOT	NOT	NOT	NOT				
100m	SIG	SIG	SIG	SIG	SIG	SIG	SIG	SIG	SIG	NOT	NOT	NOT	NOT			
10mBE	SIG	SIG	SIG	SIG	SIG	SIG	NOT	NOT	NOT	NOT	NOT	NOT	SIG	NOT		
30mBE	SIG	SIG	SIG	SIG	SIG	SIG	NOT	NOT	NOT	NOT	NOT	NOT	NOT	NOT	NOT	
100mBE	SIG	SIG	SIG	SIG	SIG	SIG	NOT	NOT	NOT	NOT	NOT	NOT	NOT	NOT	NOT	NOT

-6dB Threshold

	1m	2m	4m	5m	10m	15m	20m	25m	30m	40m	50m	75m	100m	10mBE	30mBE	100mBE
1m	NOT															
2m	NOT	NOT														
4m	NOT	NOT	NOT													
5m	NOT	NOT	NOT	NOT												
10m	NOT	NOT	NOT	NOT	NOT											
15m	NOT	NOT	NOT	NOT	NOT	NOT										
20m	NOT	SIG	NOT	SIG	NOT	NOT	NOT									
25m	NOT	SIG	NOT	SIG	NOT	NOT	NOT	NOT								
30m	NOT	SIG	NOT	SIG	NOT	NOT	NOT	NOT	NOT							
40m	SIG	SIG	SIG	SIG	SIG	SIG	SIG	SIG	SIG	NOT						
50m	SIG	SIG	SIG	SIG	SIG	SIG	SIG	SIG	SIG	NOT	NOT					
75m	SIG	SIG	SIG	SIG	SIG	NOT	NOT	NOT	NOT	NOT	NOT	NOT				
100m	SIG	SIG	SIG	SIG	SIG	SIG	SIG	SIG	SIG	NOT	NOT	NOT	NOT			
10mBE	SIG	SIG	SIG	SIG	SIG	SIG	NOT	SIG	NOT	NOT	NOT	NOT	NOT	NOT		
30mBE	SIG	SIG	SIG	SIG	SIG	SIG	SIG	SIG	SIG	NOT	NOT	NOT	NOT	NOT	NOT	
100mBE	SIG	SIG	SIG	SIG	SIG	SIG	SIG	SIG	SIG	NOT	NOT	NOT	NOT	NOT	NOT	NOT

-9dB Threshold

	1m	2m	4m	5m	10m	15m	20m	25m	30m	40m	50m	75m	100m	10mBE	30mBE	100mBE
1m	NOT															
2m	NOT	NOT														
4m	NOT	NOT	NOT													
5m	NOT	NOT	NOT	NOT												
10m	NOT	NOT	NOT	NOT	NOT											
15m	NOT	NOT	NOT	NOT	NOT	NOT										
20m	NOT	SIG	NOT	SIG	NOT	NOT	NOT									
25m	NOT	NOT	NOT	NOT	NOT	NOT	NOT	NOT								
30m	NOT	NOT	NOT	SIG	NOT	NOT	NOT	NOT	NOT							
40m	SIG	SIG	SIG	SIG	SIG	SIG	SIG	SIG	SIG	NOT						
50m	SIG	SIG	SIG	SIG	SIG	SIG	SIG	SIG	SIG	NOT	NOT					
75m	SIG	SIG	SIG	SIG	SIG	SIG	NOT	NOT	NOT	NOT	NOT	NOT				
100m	SIG	SIG	SIG	SIG	SIG	SIG	SIG	SIG	SIG	NOT	NOT	NOT	NOT			
10mBE	SIG	SIG	SIG	SIG	SIG	SIG	NOT	SIG	SIG	NOT	NOT	NOT	NOT	NOT		
30mBE	SIG	SIG	SIG	SIG	SIG	SIG	SIG	SIG	SIG	NOT	NOT	NOT	NOT	NOT	NOT	
100mBE	SIG	SIG	SIG	SIG	SIG	SIG	SIG	SIG	SIG	NOT	NOT	NOT	NOT	NOT	NOT	NOT

-12dB Threshold

	1m	2m	4m	5m	10m	15m	20m	25m	30m	40m	50m	75m	100m	10mBE	30mBE	100mBE
1m	NOT															
2m	NOT	NOT														
4m	NOT	NOT	NOT													
5m	NOT	NOT	NOT	NOT												
10m	NOT	NOT	NOT	NOT	NOT											
15m	NOT	NOT	NOT	NOT	NOT	NOT										
20m	SIG	SIG	NOT	SIG	SIG	NOT	NOT									
25m	SIG	SIG	NOT	SIG	SIG	NOT	NOT	NOT								
30m	SIG	SIG	NOT	SIG	NOT	NOT	NOT	NOT	NOT							
40m	SIG	SIG	SIG	SIG	SIG	SIG	SIG	SIG	SIG	NOT						
50m	SIG	SIG	SIG	SIG	SIG	SIG	SIG	SIG	SIG	NOT	NOT					
75m	SIG	SIG	SIG	SIG	SIG	SIG	NOT	NOT	NOT	NOT	NOT	NOT				
100m	SIG	SIG	SIG	SIG	SIG	SIG	SIG	SIG	SIG	NOT	NOT	NOT	NOT			
10mBE	SIG	SIG	SIG	SIG	SIG	SIG	SIG	SIG	SIG	NOT	NOT	NOT	NOT	NOT		
30mBE	SIG	SIG	SIG	SIG	SIG	SIG	SIG	SIG	SIG	NOT	NOT	NOT	NOT	NOT	NOT	
100mBE	SIG	SIG	SIG	SIG	SIG	SIG	SIG	SIG	SIG	NOT	NOT	NOT	NOT	NOT	NOT	NOT

Visibility Threshold

Vita

Jason Michael Cash

Jason Cash was born on August 22nd, 1977 in Newport News, Virginia. He graduated from Menchville High School in 1995 and went on to attend college at Virginia Tech in Blacksburg, Virginia where he received a Bachelor of Science in Psychology in 1999. In the spring of 2001 Jason was accepted into a graduate program at Virginia Tech in the Geography department with an interest in geographic information systems. While working on his Masters degree, Jason was fortunate enough to take an intensive summer course, Geographic Engineering Tool for Wireless: Evaluation of Broadband Systems (GETWEBS), which encouraged students from a variety of backgrounds to work together in developing a wireless communications model for Montgomery County, VA. This initial interest in wireless telecommunications would be enhanced by an offer from Virginia Tech's Center for Wireless Telecommunication's (CWT) research group for a yearlong assistantship. As a GIS analyst for the CWT, he worked on a feasibility study for LMDS communication in the Town of Grundy, VA. After completing his research with the CWT, Jason worked as a teaching assistant for the department's Introduction to GIS course, where he conducted labs and helped students work with the latest GIS software. Jason also worked part-time for the Virginia Primary Care Association (VPCA), an agency that works to provide free health care to underserved parts of the state, where he produced a variety of maps that helped the association in their cause. In May of 2003, Jason received a Master of Science degree in Geography with a focus on geographic information systems.